Quarkonia and quantum chromodynamics

W. Buchmüller
*Fermi National Accelerator Laboratory, P.O. Box 500, Batavia, Illinois 60510**

S.-H. H. Tye
Newman Laboratory of Nuclear Studies, Cornell University, Ithaca, New York 14853

(Received 19 January 1981)

The ψ and Υ spectroscopies are analyzed in the framework of a recently proposed potential model which incorporates linear confinement and asymptotic freedom. Given the Regge slope α' (α' taken to be 1 GeV^{-2}) and the quantum-chromodynamics (QCD) scale parameter Λ ($\Lambda_{\overline{\rm MS}}$ taken to be 0.5 GeV, where $\overline{\rm MS}$ refers to the modified minimal-subtraction scheme) the potential is completely determined. Excellent agreement with experiment is found, including in particular leptonic widths and hyperfine splittings. This supports a short-distance behavior of the quark-antiquark potential as predicted by QCD. We also demonstrate in a model-independent way that the Ψ and Υ spectra provide a lower bound on the QCD scale parameter Λ; we find $\Lambda_{\overline{\rm MS}} > 0.1$ GeV. The properties of $(b\bar{c})$ and possible $(t\bar{t})$, $(t\bar{c})$, and $(t\bar{b})$ spectroscopies are studied, including weak-interaction effects. The implications of the Ψ', Υ', and possible heavier quarkonium families for quantitative tests of QCD are discussed. It is shown that a $(t\bar{t})$ system with $m(t\bar{t}) \geq 40$ GeV would provide an accurate determination of $\Lambda_{\overline{\rm MS}}$.

I. INTRODUCTION

Around the time of the discovery of the J/ψ resonance[1] in 1974, Appelquist and Politzer[2] were led by the idea of asymptotic freedom to suggest that heavy quarks would form nonrelativistic positroniumlike bound states, which should be observed as narrow resonances. Since then the charmonium model[2] has been extensively developed, motivated by the hope to gain insight into the fundamental theory of strong interactions by studying their "hydrogen atom."[3]

Over the past six years, a successful description of the ψ and Υ families[4-7] has been achieved, and many predictions[3,8,9] of the charmonium model have been confirmed experimentally. Theoretical efforts have been concentrated on the exploration of specific potential models as well as the application of rigorous methods derived from nonrelativistic quantum mechanics.[10,11] The result of these efforts (with respect to the static quark-antiquark potential) is summarized in Fig. 1, where various phenomenologically successful potentials are shown. In the region $0.1\ \text{fm} \lesssim r \lesssim 1.0$ fm, which is probed by present quarkonium families, a flavor-independent[16] potential has emerged, which appears to be determined by experimental data. At large and short distances, however, a variety of asymptotic behaviors have been suggested, all of which seem to be compatible with present experimental data.

Theoretically, based on strong- and weak-coupling expansions in quantum chromodynamics (QCD), one expects the static $(Q\bar{Q})$ potential to be Coulombic at short distances and to grow linearly at large distances. The potential, obtained by a simple superposition of both asymptotic limits, has been studied extensively by the Cornell group,[15] resulting in a successful description of the ψ and Υ families. More recently various authors have investigated potentials which incorporate logarithmic modifications[17] of the Coulombic part at short distances due to vacuum-polarization effects in QCD.

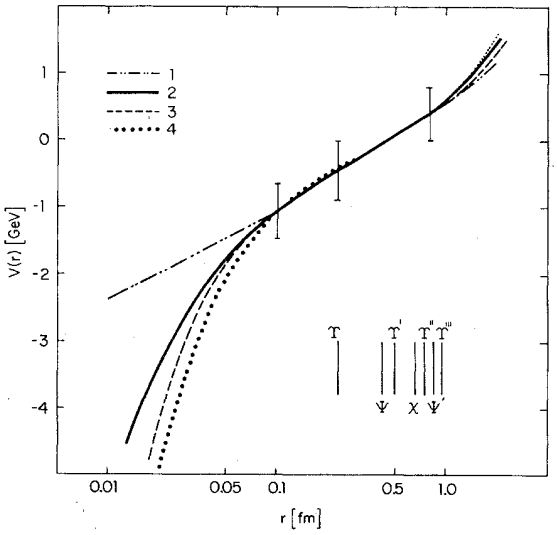

FIG. 1. Various successful potentials are shown. The numbers refer to the following references: (a) Martin, Ref. 12; (2) Buchmüller, Grunberg, and Tye, Ref. 13; (3) Bhanot and Rudaz, Ref. 14; (4) Cornell group, Ref. 15. The potentials (1), (3), and (4) have been shifted to coincide with (2) at $r = 0.5$ fm; the "error bars" indicate the uncertainty in absolute, r-independent normalization. States of the ψ and Υ families are displayed at their mean-square radii.

 © 1981 The American Physical Society

Richardson,[17] in particular, has put forward a simple and elegant ansatz which provides an excellent description of the $(c\bar{c})$ and $(b\bar{b})$ spectra and incorporates asymptotic freedom qualitatively.

Recently, we[13] have examined the relationships between the Regge slope α', the QCD scale parameter Λ, and the quarkonium potential, which we studied in terms of its dimensionless β function. These investigations led to further insight into the nature of Richardson's potential and to a new β function which possesses the asymptotic behavior at small coupling constants as required by perturbative QCD to two loops. The two-loop contribution to the β function and the one-loop correction to the potential have to be incorporated consistently, in order to relate the short-distance behavior of the quark-antiquark potential to a well-defined QCD scale parameter, say $\Lambda_{\overline{\rm MS}}$.[18] These considerations led us to a new quarkonium potential[13] which agrees numerically with Richardson's potential (as well as other potentials shown in Figs. 1 and 2) for distances probed by the ψ and Υ families. At shorter distances, however, differences among the various potentials become substantial. These lead to predictions for heavier quarkonium systems which differ significantly among the various potential models. The present work is a detailed study of the ψ, Υ, and possible heavier quarkonium systems in the framework of QCD-like potential models, especially the one proposed in Ref. 13.

In principle, given the Regge slope α' (e.g., α' taken from light-hadron spectroscopy) and the QCD scale parameter Λ (e.g., $\Lambda_{\overline{\rm MS}}$ obtained from deep-inelastic scattering experiments), our potential is completely determined. This is in contrast to other models where free parameters of the potential are determined using quarkonium data. In practice it turns out that quarkonium spectra give us a more accurate determination of α' and $\Lambda_{\overline{\rm MS}}$ in our potential model. The resulting values of α' and $\Lambda_{\overline{\rm MS}}$ are 1 GeV^{-2} and 0.5 GeV, respectively (due to the different number of effective flavors for quarkonia and light hadrons as well as other uncertainties, we expect that different determinations of α' should agree to only within 20%).

However, even if one accepts the success of QCD-like models, the question remains whether these achievements really provide evidence in favor of theoretical expectations based on QCD or whether they just demonstrate their consistency with experimental data. These doubts are enhanced by the success of a class of essentially logarithmic potentials,[10,19] investigated in great detail by Quigg and Rosner, and Martin,[12] which have no resemblance with the theoretically expected asymptotic behaviors at either small or large distances.

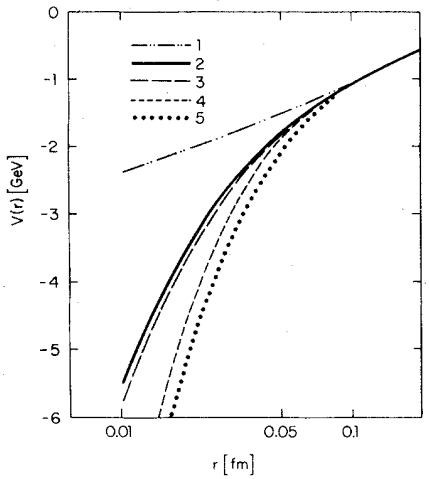

FIG. 2. The short-distance behavior of various potentials is shown. The numbers refer to the following references: (1) Martin, Ref. 12; (2) Buchmüller, Grunberg, and Tye, Ref. 13; (3) Richardson, Ref. 17; (4) Bhanot and Rudaz, Ref. 14; (5) Cornell group, Ref. 15.

In this paper we address ourselves to the question of what we can learn from quarkonia about asymptotic freedom and QCD in general. Our analysis shows that a heavy quarkonium system of mass $m \geq 40$ GeV would clearly distinguish between the various potential models. It would probe the $(Q\bar{Q})$ potential at sufficiently short distances to test the prediction of perturbative QCD, and it would also provide a clean determination of the scale parameter Λ. In view of the various theoretical and experimental uncertainties in the application of perturbative QCD to deep-inelastic scattering and other processes, an independent determination of the Λ parameter in QCD by means of heavy quarkonia would be of great importance. The quantities which are most sensitive to the short-distance part of the $(Q\bar{Q})$ potential are leptonic widths[20] and hyperfine splittings. Our analysis of the ψ and Υ families leads to the theoretical predictions (cf. Sec. III)

$$\Gamma_{ee}(\Upsilon) = 1.07 \pm 0.24 \text{ keV}$$

and

$$\Delta E_{\psi - \eta_c} = 99 \text{ MeV}.$$

The agreement of these results with experimental data supports a short-distance behavior of the quark-antiquark potential as predicted by QCD. Furthermore, the numerical values for the Regge slope and the QCD scale parameter, $\alpha' \simeq 1$ GeV^{-2} and $\Lambda_{\overline{\rm MS}} \simeq 0.5$ GeV, are in quantitative

agreement with results obtained from light-hadron spectroscopy and deep-inelastic scattering experiments.

The paper is organized as follows. In Sec. II we review the basic theoretical expectations concerning heavy-quark–antiquark bound states. Section III deals with the $(c\bar{c})$, $(b\bar{b})$, and $(b\bar{c})$ families in the framework of a specific potential model which incorporates asymptotic freedom and linear confinement. In Sec. IV we discuss in a model-independent way the implications of present and (hopefully) future quarkonium systems for quantitative tests of QCD. Section V is devoted to a study of $(t\bar{t})$, $(t\bar{c})$, and $(t\bar{b})$ spectroscopies, and in Sec. VI weak-interaction (i.e., Z-boson) effects are briefly discussed. In Sec. VII we summarize our results and comment on remaining problems. Appendix A deals with details of the potential used, and in Appendix B we give a brief discussion of QCD corrections to leptonic widths and the origin of the various uncertainties involved.

II. THE STATIC $(Q\bar{Q})$ POTENTIAL AND ASYMPTOTIC FREEDOM

At present a theory of bound states in QCD does not exist, and even its nonrelativistic limit, which should be applicable for heavy-quark–antiquark systems, cannot be derived from first principles. One therefore has to start from a set of reasonable theoretical expectations, which will (hopefully) be put on a firm theoretical basis in the future. Our theoretical expectations are the following.

(1) The mass spectrum of heavy-quark–antiquark bound states has the form

$$M_n(Q\bar{Q}) = 2m_Q + E_n(m_Q, V), \tag{2.1}$$

where m_Q is the quark mass and $E_n(m_Q, V)$ is the energy eigenvalue of the nonrelativistic Schrödinger equation with a flavor-independent potential $V(\vec{r})$.

(2) The asymptotic limits of the static $(Q\bar{Q})$ potential read

$$V(r) \underset{r\to\infty}{\sim} kr, \tag{2.2a}$$

$$V(r) \underset{r\to 0}{\sim} \frac{1}{r\ln(1/\Lambda^2 r^2)}\left[1 + O\left(\frac{1}{\ln(1/\Lambda^2 r^2)}\right)\right], \tag{2.2b}$$

where k is the string tension and Λ the QCD scale parameter.

(3) In order to relate these asymptotic behaviors to experimental data, one has to specify at what distances corrections to Eqs. (2.2) are expected to be negligible. For the lack of a more definite criterion we choose, at short distances,

$$r \leq r_c, \quad \frac{1}{r_c^2 \Lambda_{\overline{\rm MS}}^2} = 100, \tag{2.3}$$

in accord with analyses of deep-inelastic scattering processes where, for momentum transfers Q with $|Q|^2 \geq Q_c^2$, $Q_c^2/\Lambda_{\overline{\rm MS}}^2 = 100$, perturbative calculations are considered to be reliable.[21]

The static $(Q\bar{Q})$ potential $V(\vec{r})$ is a quantity that has the dimensions of mass. It depends on dimensionless parameters (e.g., group factors) characterizing the QCD Lagrangian and (if the masses of light quarks can be neglected) a single scale which we may choose to be Λ or the string tension k. In order to disentangle these two ingredients which determine the $(Q\bar{Q})$ interaction it is useful to look at the dimensionless β function of the running coupling constant related to the potential. This is the approach of Ref. 13, which we shall now review.

Let us consider the Fourier transform of $V(\vec{r})$ and define a physical running coupling constant $\rho(Q^2)$, $\rho = g^2/16\pi^2 = \alpha_s/4\pi$, (for momentum transfer $\vec{Q}$, $Q^2 \equiv \vec{Q}^2$) as

$$V(Q^2) = -\frac{16\pi^2 C_2(R)\rho(Q^2)}{Q^2}, \tag{2.4}$$

where the group factor $C_2(R)$ equals $\frac{4}{3}$ in QCD.[22] We emphasize that $\rho(Q^2)$ is a physical quantity and therefore independent of the choice of gauge and the subtraction scheme. For large values of Q^2, perturbative QCD implies

$$\rho(Q^2) \underset{Q^2\to\infty}{\sim} \frac{1}{b_0 \ln(Q^2/\Lambda^2)} - \frac{b_1}{b_0^3}\frac{\ln\ln(Q^2/\Lambda^2)}{\ln^2(Q^2/\Lambda^2)} + O\left(\frac{1}{\ln^3(Q^2/\Lambda^2)}\right), \tag{2.5a}$$

where[23]

$$b_0 = \tfrac{11}{3}C_2(G) - \tfrac{2}{3}N_f,$$
$$b_1 = \tfrac{34}{3}[C_2(G)]^2 - \tfrac{10}{3}C_2(G)N_f - 2C_2(R)N_f. \tag{2.5b}$$

For small Q^2 one obtains from Eq. (2.2a)

$$\rho(Q^2) \underset{Q^2\to 0}{\sim} \frac{K}{Q^2}[1 + o(1)]. \tag{2.5c}$$

The β function related to the running coupling constant $\rho(Q^2)$ is given by

$$\beta(\rho) = Q^2 \frac{\partial}{\partial Q^2}\rho(Q^2)\Big|_{Q^2 = Q^2(\rho)}, \tag{2.6}$$

and from Eqs. (2.5) we read off its asymptotic behaviors,

$$\beta(\rho) \underset{\rho\to 0}{\sim} -b_0\rho^2 - b_1\rho^3 + O(\rho^4), \tag{2.7a}$$

$$\beta(\rho) \underset{\rho\to\infty}{\sim} -\rho[1+o(1)]. \tag{2.7b}$$

Using the boundary conditions Eqs. (2.5) for both large and small values of Q^2, the running coupling constant can be expressed in terms of the β function:

$$\ln\frac{Q^2}{\Lambda^2} = \frac{1}{b_0\rho} + \frac{b_1}{b_0^2}\ln(b_0\rho) + \int_0^\rho dx\left[\frac{1}{b_0x^2} - \frac{b_1}{b_0^2}\frac{1}{x} + \frac{1}{\beta(x)}\right], \tag{2.8a}$$

and

$$\ln\frac{K}{Q^2} = \ln\rho + \int_\rho^\infty dx\left[\frac{1}{x} + \frac{1}{\beta(x)}\right]. \tag{2.8b}$$

Equations (2.8) are uniquely determined by specifying the asymptotic limits of $\rho(Q^2)$, as given by Eqs. (2.5), and by the requirement that the occurring integrals are finite. In particular, the integral over the inverse β function in Eq. (2.8a) is well defined only after the one- and two-loop contributions have been subtracted. The sum of Eqs. (2.8a) and (2.8b) reads

$$\ln\frac{K}{\Lambda^2} = \frac{1}{b_0\rho} + \frac{b_1}{b_0^2}\ln(b_0\rho) + \int_0^\rho dx\left[\frac{1}{b_0x^2} - \frac{b_1}{b_0^2}\frac{1}{x} + \frac{1}{\beta(x)}\right] + \ln\rho + \int_\rho^\infty dx\left[\frac{1}{x} + \frac{1}{\beta(x)}\right], \tag{2.8c}$$

where the explicit dependence on Q^2 has dropped out. Since the running coupling ρ is a function of Q^2, self-consistency requires the right-hand side of Eq. (2.8c) to be independent of ρ. A simple examination shows that this is indeed the case. For convenience, we shall put $\rho=1$ in Eq. (2.8c) for later use.

In order to relate the scale parameter Λ in Eqs. (2.5) and (2.8) to the Λ parameter in a specific regularization scheme, one has to calculate the complete one-loop contribution to the static $(Q\bar{Q})$ potential. For the $\overline{\text{MS}}$ scheme one obtains [13,24,25]

$$\ln\frac{\Lambda}{\Lambda_{\overline{\text{MS}}}} = \frac{1}{2b_0}\left(\tfrac{31}{9}C_2(G) - \tfrac{10}{9}N_f\right). \tag{2.9}$$

The relation between the constant K in Eq. (2.8b), the string tension k and the asymptotic Regge slope α' is given by

$$\alpha' = \frac{1}{2\pi k} = \frac{1}{4\pi^2 C_2(R)K}. \tag{2.10}$$

The combination of Eqs. (2.8), (2.9), and (2.10) leads to an expression of the dimensionless quantity $\alpha'\Lambda_{\overline{\text{MS}}}^2$ in terms of the β function[13]

$$\ln(\alpha'\Lambda_{\overline{\text{MS}}}^2) = -\ln[4\pi^2C_2(R)] - \frac{1}{b_0}\left(\tfrac{31}{9}C_2(G) - \tfrac{10}{9}N_f\right) - \frac{1}{b_0} - \frac{b_1}{b_0^2}\ln b_0 - \int_0^1 dx\left(\frac{1}{b_0x^2} - \frac{b_1}{b_0^2x} + \frac{1}{\beta(x)}\right) - \int_1^\infty dx\left(\frac{1}{x} + \frac{1}{\beta(x)}\right). \tag{2.11}$$

Obviously, the β function determines the relation between α' and $\Lambda_{\overline{\text{MS}}}$. Setting the scale of the theory by fixing α' or $\Lambda_{\overline{\text{MS}}}$, one obtains the $(Q\bar{Q})$ potential via Eqs. (2.8) and (2.4).

In principle, the β function can be evaluated directly from QCD. At present, however, this has not been achieved and only the asymptotic limits, corresponding to the leading contributions in weak- and strong-coupling expansions, are known theoretically. However, any interpolation between these two asymptotic regimes is restricted empirically at intermediate coupling strengths by the requirement that the resulting potential has to provide a description of the ψ and Υ spectroscopies. An example[13] which satisfies this condition is given by

$$\frac{1}{\beta(\rho)} = -\frac{1}{b_0\rho^2(1-e^{-1/b_0\rho})} + \frac{b_1}{b_0^2}\frac{1}{\rho}e^{-l\rho}, \tag{2.12}$$

where $\beta(\rho)$ approaches

$$\beta(\rho) \underset{\rho\to0}{\sim} -b_0\rho^2 - b_1\rho^3 - \frac{b_1(b_1-lb_0)}{b_0}\rho^4 + O(\rho^5)$$

and

$$\beta(\rho) \underset{\rho\to\infty}{\sim} -\rho + \frac{1}{2b_0} + O\left(\frac{1}{\rho}\right).$$

We note that l is related to the three-loop contribution to $\beta(\rho)$. So far this coefficient has not been calculated, and therefore we treat l as a

free parameter. From the ψ and Υ spectra we infer $l=24$. An immediate consequence of this choice of the β function is the relation between the Regge slope α' and the scale parameter Λ. Carrying out the integrations in Eq. (2.11) yields

$$\ln\alpha'\Lambda_{\overline{\rm MS}}^2 = -\ln[4\pi^2 C_2(R)] + \ln b_0 + \frac{b_1}{b_0^2}\left(\gamma_E + \ln\frac{l}{b_0}\right) - \frac{1}{b_0}\left[\tfrac{31}{9}C_2(G) - \tfrac{10}{9}N_f\right], \quad (2.13)$$

where $\gamma_E = 0.5772\ldots$ is Euler's constant. For QCD with three flavors one obtains $\alpha'\Lambda_{\overline{\rm MS}}^2 = 0.27$, i.e., a Regge slope of $\alpha' \sim 1$ GeV^{-2} corresponds to a scale parameter $\Lambda_{\overline{\rm MS}} \sim 500$ MeV.

The β function characterizing Richardson's potential can be recovered in two ways. One possibility is to neglect the two-loop contribution at small coupling strengths, i.e., $b_1 = 0$. The intriguing feature of the resulting β function,

$$\beta^{\rm Rich}(\rho) = -b_0\rho^2(1 - e^{-1/b_0\rho}),$$

is the essential singularity at $\rho = 0$. Precisely this structure is expected if classical field configurations[26] are important for the transition[27] between weak- and strong-coupling regimes. The other way to recover Richardson's potential is to take the limit $l \to \infty$ in Eq. (2.12). It is obvious from Eq. (2.13) that $\Lambda_{\overline{\rm MS}}$ becomes infinite in this limit if the Regge slope α' is kept fixed. It is therefore not possible to infer a well-defined QCD scale parameter Λ from Richardson's potential. It may rather be considered as the limiting case obtained as $\Lambda_{\overline{\rm MS}}$ approaches infinity (cf. Sec. V).

The term proportional to b_1 in Eq. (2.12) is relevant only for small values of ρ due to the large negative coefficient in the exponential function. The potential which results from Eq. (2.12) differs therefore from Richardson's potential only at small values of the running coupling constant, i.e., at short distances (cf. Fig. 2). These differences, however, lead to substantially different predictions for heavier quarkonium spectroscopies which we will investigate in Sec. V.

A comment on the β function defined in Eqs. (2.4) and (2.6) is in order. The Callan-Symanzik β function in the Gell-Mann–Low renormalization-group approach is defined within the perturbative formalism (order by order to all orders). To two loops the β function is universal, i.e., renormalization-scheme-independent, and gauge-invariant. Its three-loop and higher-order contributions are in general gauge-dependent and scheme-dependent. In contrast, we have defined the β function in terms of a physical coupling constant, which is directly measurable in experiments. Consistency implies that our definition of the β function must be gauge- and scheme-independent. Also this definition does not require the β function to have a small coupling perturbative expansion [in fact, the β function in Eq. (2.12) has an essential singularity at $\rho = 0$, so that its expansion around $\rho = 0$ is only an asymptotic series]. As is clear from Eq. (2.8a) the scale parameter Λ is defined after two subtractions which involve the coefficients b_0 and b_1. In order for Λ to have a well defined meaning the coefficients b_0 and b_1 have to be universal. Our β function is, of course, "process-dependent"; it is defined in terms of a particular physical quantity, the quark-antiquark potential. Clearly the corresponding definition is also useful for other scattering processes.

To conclude this section let us emphasize that the choice of the β function in Eq. (2.12) is by no means unique. Its appealing features are the asymptotic limits for small and large values of ρ (as expected on the basis of QCD), its interesting analytic structure at $\rho = 0$ (inherent in Richardson's potential), and its simplicity. The reader is invited to find other examples which meet these criteria and provide an adequate description of the ψ and Υ spectroscopies.

III. $(c\bar{c})$ AND $(b\bar{b})$ SPECTROSCOPIES

In Sec. II we have reviewed the theoretical framework for the description of heavy-quark bound states, and we have discussed how to incorporate asymptotic freedom in the $(Q\bar{Q})$ interaction. Given the β function of Eq. (2.12) and the Regge slope $\alpha' \simeq 1$ GeV^{-2}, the $(Q\bar{Q})$ potential is determined via Eqs. (2.4) and (2.8). Equation (2.11) implies $\alpha'\Lambda_{\overline{\rm MS}}^2 = 0.27$, from which one obtains for the scale parameter $\Lambda_{\overline{\rm MS}} \simeq 0.5$ GeV.

A. Mass spectra

Tables I and II summarize, for spin-triplet states of the ψ and Υ families, mass spectra, ratios of leptonic widths, velocities, and mean-

TABLE I. $(c\bar{c})$ spectrum: masses, ratios of leptonic widths, velocities, and mean-square radii. The mass of the ground state is input; it determines the c-quark mass $m_c = 1.48$ GeV.

State	Mass (GeV)	$\Gamma_{ee}/\Gamma_{ee}(1S)$	$\langle v^2/c^2\rangle$	$\langle r^2\rangle^{1/2}$ (fm)
$1S$	3.10	1	0.23	0.42
$1P$	3.52		0.25	0.67
$2S$	3.70	0.46	0.29	0.85
$1D$	3.81		0.29	0.87
$2P$	3.97		0.32	1.05
$3S$	4.12	0.32	0.36	1.20
$2D$	4.19		0.36	1.22
$4S$	4.48	0.25	0.44	1.48

TABLE II. $(b\bar{b})$ spectrum: masses, ratios of leptonic widths, velocities, and mean-square radii. The mass of the ground state is input; it determines the b-quark mass $m_b = 4.88$ GeV. With respect to the CESR normalization, $M(\Upsilon) = 9.433$ (Ref. 7), the b-quark mass is given by $m_b = 4.87$ GeV, and the masses of excited states are smaller by 27 (MeV).

State	Mass (GeV)	$\Gamma_{ee}/\Gamma_{ee}(\Upsilon)$	$\langle v^2/c^2 \rangle$	$\langle r^2 \rangle^{1/2}$ (fm)
$1S$	9.46	1	0.077	0.23
$1P$	9.89		0.069	0.39
$2S$	10.02	0.44	0.075	0.50
$1D$	10.14		0.072	0.53
$2P$	10.25		0.078	0.65
$3S$	10.35	0.32	0.085	0.75
$2D$	10.43		0.083	0.77
$3P$	10.53		0.090	0.87
$4S$	10.62	0.26	0.098	0.95
$3D$	10.68		0.098	0.97
$5S$	10.86	0.25	0.13	1.1

square radii of the bound constituents which follow from the given potential and the relation Eq. (2.1) between masses and energy eigenvalues of the Schrödinger equation. The agreement with experiment is satisfactory. The computed masses coincide with the experimentally measured[8] ones within 10 MeV, except for the $4S$ state in the Υ family, where the disagreement is 40 MeV. This state, however, lies above the threshold for $B\bar{B}$ production, its width is about 20 MeV, and corrections due to coupled-channel effects are expected to be important. The only free parameters adjusted to obtain these results are the masses of the c and b quarks. They are determined by identifying the $1S$ states with the ψ and Υ resonances.

B. Leptonic widths

In the framework of the potential model, the leptonic widths of the S states are given by[28]

$$\Gamma_{ee}(nS) = \frac{16\pi e_Q^2 \alpha^2}{M_n^2(Q\bar{Q})} |\psi_n(0)|^2 \equiv \Gamma_{ee}^{(0)}(nS). \quad (3.1)$$

In QCD, Eq. (3.1) is modified by radiative[29] and relativistic corrections,

$$\Gamma_{ee} = \Gamma_{ee}^{(0)}\left(1 - \frac{16}{3\pi}\alpha_s(2m_Q) \pm \Delta\right). \quad (3.2)$$

The leading radiative correction can be calculated reliably in perturbation theory, whereas higher-order radiative and relativistic corrections lead to an uncertainty Δ [a discussion of Eq. (3.2) is given in Appendix B]. Guided by our experience with nonrelativistic bound states in quantum electrodynamics, the order of magnitude of Δ can be estimated as follows.

(i) There will be higher-order radiative corrections, and we assume their coefficient to be of the same order of magnitude as the lowest-order coefficient, i.e., $\Delta^{\rm rad} = (16/3\pi)\alpha_s^2$.

(ii) For Coulombic bound states relativistic corrections, which are of order v^2/c^2, are also proportional to α^2 and usually not distinguished from radiative corrections. However, the ψ and Υ families are not Coulombic bound states, and we therefore include an additional uncertainty $\Delta^{\rm rel} = v^2/c^2$. Using the running coupling constant for $\Lambda_{\overline{\rm MS}} = 0.5$ GeV (cf. Fig. 3) and the values of v^2/c^2 from Tables I and II we obtain $\Delta(\psi) = 0.39$ and $\Delta(\Upsilon) = 0.15$, where $\Delta = \Delta^{\rm rad} + \Delta^{\rm rel}$. From Eq. (3.2) we thus obtain the theoretical leptonic widths

$$\Gamma_{ee}(\psi) = 3.70 \pm 3.05 \text{ keV}$$

and

$$\Gamma_{ee}(\Upsilon) = 1.07 \pm 0.24 \text{ keV},$$

where we have used $\alpha_s(3.1 \text{ GeV}) = 0.31$ and $\alpha_s(9.5 \text{ GeV}) = 0.20$ (cf. Fig. 3). The measured leptonic widths for the Υ read[7]

CLEO[7]: 1.02 ± 0.22 keV,

CUSB[7]: 1.07 ± 0.23 keV,

DORIS[5]: 1.29 ± 0.22 keV.

The uncertainties quoted for the theoretical leptonic widths of ψ and Υ involve estimates of relativistic and radiative corrections. For ratios of leptonic widths of states in the same

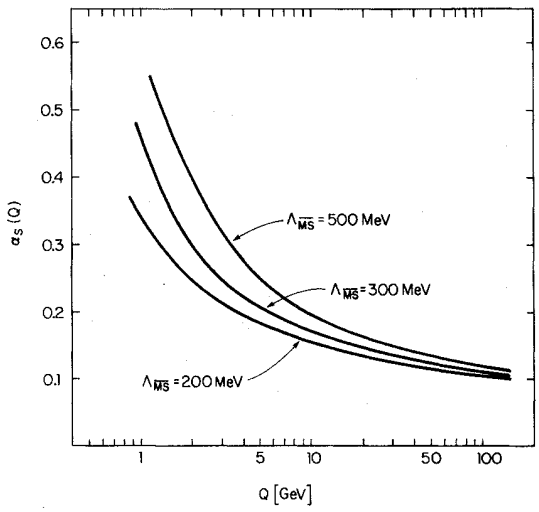

FIG. 3. The running coupling constant $\alpha_s(Q)$ in QCD with four flavors for different values of $\Lambda_{\overline{\rm MS}}$. The two-loop contribution of the β function is included, i.e.,

$$\alpha_s(Q) = \frac{12\pi}{25}\frac{1}{\ln(Q^2/\Lambda_{\overline{\rm MS}}^2)}\left(1 - \frac{462}{625}\frac{\ln\ln(Q^2/\Lambda_{\overline{\rm MS}}^2)}{\ln(Q^2/\Lambda_{\overline{\rm MS}}^2)}\right).$$

family the radiative corrections cancel. The relativistic corrections, however, will in general depend on the principal quantum number, i.e., they will not completely cancel. In the ψ family we therefore expect uncertainties of about 30% for ratios of leptonic widths, whereas in the Υ family relativistic corrections should be less than 10%.

C. Hyperfine splittings

So far no completely satisfying theoretical description of the fine and hyperfine structure in charmonium[8,30] has been achieved. Due to the Thomas precession the fine structure will necessarily involve long-distance effects and may therefore be difficult to understand in the framework of the potential model. It is conceivable, however, that the hyperfine splitting is entirely a short-distance effect which can be calculated in perturbation theory. To first order in α_s the Hamiltonian[30] reads

$$H_{\mathrm{HFS}} = \frac{8\pi}{3} C_2(R) \frac{\alpha_s}{m_Q^2} \vec{S}_1 \cdot \vec{S}_2 \delta^3(\vec{r}) . \tag{3.3}$$

As our model accounts correctly for the leptonic widths without any "normalization factor," we have no reason to invoke a similar factor in Eq. (3.3) and the hyperfine splittings are uniquely determined. For the ψ-η_c splitting we obtain [α_s (3.1 GeV) = 0.31, cf. Fig. 3]

$$\Delta E^{\mathrm{th}}_{\psi-\eta_c} = 99 \text{ MeV},$$

which compares well with the measured[31] value

$$\Delta E^{\mathrm{exp}}_{\psi-\eta_c} = 119 \pm 9 \text{ MeV}.$$

It is interesting to compare the theoretical predictions for the hyperfine splittings and the leptonic widths, both of which are proportional to the square of the wave function at the origin. Compared to the experimental value, the lowest-order leptonic width for the ψ is too large by 62% and is reduced via first-order QCD corrections by 85%. On the contrary, the lowest-order hyperfine splitting is too small by only 16%. First-order QCD corrections are therefore expected to be small. Their calculation is in progress,[32] and the result will provide a further test for QCD-like potential models.

In Table III we have listed predictions, based on Eq. (3.3), for the hyperfine splittings in the ψ and Υ families. In the derivation of the Hamiltonian Eq. (3.3), binding effects are neglected, i.e., the quarks are considered to be on-shell. The size of binding corrections can be estimated by replacing m_Q by $\frac{1}{2}M(Q\bar{Q})$ in Eq. (3.3). They turn out to be negligible except for the ψ' where they decrease the splitting by 43% as indicated in Table III. At present there seems to be no way to resolve this theoretical ambiguity.

TABLE III. Lowest-order hyperfine splittings $\Delta E \equiv E(^3S_1) - E(^3S_0)$ in ψ and Υ families. For ψ' the number in parentheses is obtained by replacing m_Q by $\frac{1}{2}M(\psi')$ in Eq. (3.3).

State	ΔE (MeV)
ψ	99
ψ'	65 (42)
Υ	46
Υ'	23
Υ''	18

D. $E1$ transitions

The rates for $E1$ transitions[9,15,33,34] are given by

$$\Gamma_{if} = \tfrac{4}{3} e_Q^2 \alpha \omega^3 S_{if} D_{if}^2 (2j_f + 1), \tag{3.4}$$

where e_Q is the electric charge of the quark, α the fine-structure constant, and ω the energy of the emitted photon; the dipole moment D_{if} represents the overlap integral with respect to the radial wave functions,

$$D_{if} = \int_0^\infty dr R_i(r) r R_f(r),$$

where

$$\int_0^\infty dr R_f R_i = \delta_{if}, \tag{3.5}$$

and the statistical factor S_{if} for a transition $(j_i, l_i) \to (j_f, l_f)$ (j and l denote total spin and orbital angular momentum) can be expressed in terms of Wigner's 6-j symbol,[33,34]

$$S_{if} = \begin{Bmatrix} j_i & 1 & j_f \\ l_f & s & l_i \end{Bmatrix}^2 \max\{l_i, l_f\}, \tag{3.6}$$

where s denotes the spin of initial and final state. For singlet states one obtains $S_{if} = 1/(2j_i + 1)$; for triplet states the relevant values of the 6-j symbols are listed in Table IV.

Tables V and VI contain photon momenta, dipole moments, and widths for various $E1$ transitions in the ψ and Υ family. For the Υ family, the splittings of the P and D states are not included. The fine-structure splittings in the Υ family are expected to be smaller than those in the ψ family. Yet their effect on the transition rates will be very important and may easily amount to a factor of 2. For the transitions $\psi' \to \gamma\chi_J$, theory and experiment disagree by a factor of 2 to 4, and one has to expect a similar discrepancy in the Υ spectrum. We do not fully understand the origin

TABLE IV. The statistical factors

$$\frac{1}{\max\{l_i,l_f\}}S_{if}\equiv\begin{Bmatrix} j_i & 1 & j_f \\ l_f & 1 & l_i \end{Bmatrix}^2$$

for $E1$ transitions $(j_i,l_i)\longleftrightarrow(j_f,l_f)$ [cf. Eq. (3.6)]. Note the symmetry of S_{if} with respect to interchange of initial and final quantum numbers.

(j_i,l_i) \ (j_f,l_f)	$(l,l+1)$	$(l+1,l+1)$	$(l+2,l+1)$
$(l-1,l)$	$\frac{1}{(2l+1)^2}$		
(l,l)	$\frac{1}{(l+1)^2(2l+1)^2}$	$\frac{(l+2)}{(l+1)^2(2l+1)(2l+3)}$	
$(l+1,l)$	$\frac{1}{(l+1)^2(2l+1)^2(2l+3)^2}$	$\frac{1}{(l+1)^2(2l+3)^2}$	$\frac{1}{(2l+3)^2}$

of this disagreement, which is common to all potential models. One may, however, expect QCD corrections to the lowest-order contribution which are considerably larger than in the case of the leptonic widths because of the different magnitude of the photon energies involved in both cases. Clearly, the computation of relativistic and radiative corrections to the lowest-order formula for $E1$ transitions[36] is at present one of the major theoretical problems in quarkonium physics.

E. $(b\bar{c})$ mesons

Given the c- and b-quark masses as well as the $(Q\bar{Q})$ potential from the analysis of the ψ and Υ families, the spectrum of $(b\bar{c})$ mesons, which have a reduced mass m_R satisfying $\frac{1}{2}m_c<m_R<\frac{1}{2}m_b$, is uniquely determined. The properties of the lowest spin-triplet state and its first radial excitation are displayed in Table VII. Equation (3.3) implies a lowest-order hyperfine splitting of 50 MeV for the ground state. We therefore obtain for the mass of the pseudoscalar $(b\bar{c})$ ground state

$$M_{b\bar{c}}(1\,^1S_0)=6.29\ \text{GeV}\,.$$

The $(b\bar{c})$ system probes the quarkonium potential at distances where it is already determined from the analysis of the ψ and Υ families. Any model which describes the ψ and Υ spectroscopies should therefore yield the same predictions for the $(b\bar{c})$ system. This is indeed the case, and the results presented in this section can be regarded as firm. Similar values for $(b\bar{c})$ masses have been obtained by others.[37]

TABLE V. Lowest-order rates for $E1$ transitions in ψ family. Photon momenta are computed from the measured masses of the χ states: $M(\chi_0)=3.415$ GeV, $M(\chi_1)=3.510$ GeV, $M(\chi_2)=3.550$ GeV. Experimental data are taken from Ref. 35.

Transition	k_γ (MeV)	D_{if} (fm)	Γ_{E1} (keV) Theory	Γ_{E1} (keV) Experiment
$\psi'\to\gamma\chi_0$	259	−0.517	58	15±7
$\to\gamma\chi_1$	170	−0.517	49	15±7
$\to\gamma\chi_2$	132	−0.517	38	15±7
$\chi_0\to\gamma\psi$	305	0.416	182	
$\chi_1\to\gamma\psi$	390	0.416	381	
$\chi_2\to\gamma\psi$	426	0.416	496	

IV. ASYMPTOTIC FREEDOM AND QUARKONIA

The results, which we have presented in the last section, demonstrate that a potential model, which incorporates asymptotic freedom and linear confinement, is able to provide an accurate description of the properties of the ψ and Υ spectroscopies. However, the questions remain: Is this success evidence for the theoretical expectations based on QCD or is the QCD-like potential model just one out of many different models all of which are consistent with experimental data? In par-

TABLE VI. Dipole momenta and $E1$ transitions in Υ family. The statistical factors can be obtained from Eq. (3.6) and Table IV.

Transition	k_γ (MeV)	D_{if} (fm)	$\Gamma_{E1}/3S_{if}(2j_f+1)$ (keV)
$2D\to2P$	178	0.532	14.8
$2D\to1P$	526	0.049	3.25
$3S\to2P$	100	−0.524	2.55
$3S\to1P$	450	0.002	3.10^{-3}
$2P\to1D$	109	−0.365	1.60
$2P\to2S$	227	0.382	15.9
$2P\to1S$	760	0.047	9.00
$1D\to1P$	247	0.388	21.1
$2S\to1P$	129	−0.322	2.06
$1P\to1S$	421	0.223	34.5

TABLE VII. $(b\bar{c})$ bound states: masses, wave functions at the origin, velocities, and mean-square radii.

State	Mass (GeV)	$\lvert\psi(0)\rvert^2$ (fm^{-3})	$\langle v^2/c^2\rangle$	$\langle r^2\rangle^{1/2}$ (fm)
$1S$	6.34	16.5	0.15	0.34
$2S$	6.91	9.86	0.18	0.71

ticular, what are the uncertainties in the relationship between the Regge slope and the QCD scale parameter $\alpha'\Lambda_{\overline{\rm MS}}{}^2 = 0.27$, determined from the ψ and Υ spectroscopies (as discussed in Sec. II)?

Recently, Martin[12] has given an excellent fit of the ψ and Υ mass spectra based on the potential $A + Br^{\alpha}$, $\alpha = 0.104$ (cf. Figs. 1 and 2, and Table VIII) whose asymptotic behaviors at small and large distances strongly disagree with theoretical prejudices. The results for the ratios of the leptonic widths are not as excellent as those for the energy levels; furthermore, in order to obtain the correct absolute values of the leptonic widths on the basis of a power potential one has to choose either a small value for the c-quark mass yielding results for the $E1$ transitions which are even worse than those obtained in Sec. III D, or a quark-mass dependent "correction factor" in the Van Royen–Weisskopf formula. However, due to experimental uncertainties and the lack in our theoretical understanding of relativistic corrections, both the small-power potentials as well as QCD-like models appear to be consistent with present experimental data, and the evidence for asymptotic freedom from quarkonia remains unconfirmed. As we shall discuss later, only the existence of another heavy quarkonium system would settle this issue.

It is interesting, however, that if the short-distance part of the potential is indeed determined by perturbative QCD, the ψ and Υ spectra put a lower bound on the scale parameter Λ. As we have pointed out in the introduction, the $(Q\bar{Q})$ potential appears to be determined experi-

TABLE VIII. Predictions of various potential models for the Υ family compared with experiment. Model 1: Martin (Ref. 12); model 2: Buchmüller, Grunberg, and Tye (Ref. 13), $\Lambda_{\overline{\rm MS}} = 0.5$ GeV; model 3: Richardson (Ref. 17); model 4: Bhanot and Rudaz (Ref. 14) (the range of predictions, which are dependent on the b-quark mass, is given); model 5: Cornell group (Ref. 15); model 2a: model 2 with $\Lambda_{\overline{\rm MS}} = 0.4$ GeV; model 2b: potential 2 for distances $r > 0.2$ fm, asymptotic-freedom Coulomb-type potential for $r < 0.2$ fm with $\Lambda_{\overline{\rm MS}} = 0.1$ GeV. The first column contains the leptonic widths in keV, the second and third columns the excitation energies in MeV, and, in parentheses, the ratios of the leptonic widths with respect to the Υ.

	Υ	Υ'	Υ''
Experiment			
(a) Ref. 5	1.29 ± 0.22	553 ± 10	
		(0.45 ± 0.08)	
(b) Refs. 6 and 7	1.02 ± 0.22	560 ± 3	889 ± 4
	1.07 ± 0.23	(0.45 ± 0.07)	(0.32 ± 0.06)
Model 1 (Martin)		560	890
		(0.43)	(0.28)
Model 2 (Buchmüller, Grunberg, and Tye)	1.07	555	890
		(0.46)	(0.32)
Model 3 (Richardson)		555	886
		(0.42)	(0.30)
Model 4 (Bhanot and Rudaz)	1.07–1.77	561–566	881–879
		(0.47–0.76)	(0.34–0.51)
Model 5 (Cornell group)		560	898
		(0.48)	(0.34)
Model 2a	1.03	528	857
		(0.47)	(0.34)
Model 2b	0.50	486	805
		(0.64)	(0.51)

mentally for distances 0.1 fm $\leq r \leq$ 1.0 fm (cf. Fig. 1). At short distances the Coulomb-type potential,[38] as predicted by perturbative QCD, reads

$$V_{(r)}^{\mathrm{QCD}} \underset{r\to 0}{\sim} -\frac{C_2(R)\alpha_s(r)}{r},$$

$$\alpha_s(r) = \frac{4\pi}{b_0 \ln(1/r^2\Lambda_{\overline{\mathrm{MS}}}^2)}\left[1 - \frac{b_1}{b_0^2}\frac{\ln\ln(1/r^2\Lambda_{\overline{\mathrm{MS}}}^2)}{\ln(1/r^2\Lambda_{\overline{\mathrm{MS}}}^2)} + \frac{C}{\ln(1/r^2\Lambda_{\overline{\mathrm{MS}}}^2)} + O\left(\frac{1}{\ln^2(1/r^2\Lambda_{\overline{\mathrm{MS}}}^2)}\right)\right], \tag{4.1}$$

$$C = \frac{1}{b_0}\left[\tfrac{31}{9}C_2(G) - \tfrac{10}{9}N_f\right] + 2\gamma_E,$$

where γ_E is Euler's constant. In Fig. 4 we have displayed this asymptotic freedom potential for various values of $\Lambda_{\overline{\mathrm{MS}}}$, assuming four flavors, i.e., $N_f = 4$ (for distances under consideration which satisfy $r < r_0$, $1/r_0^2 > 4m_c^2$, the effective number of flavors is $N_f = 4$; for distances $r > r_0$, the effect of changing $N_f = 4$ to $N_f = 3$ is numerically negligible for our conclusions). According to Eq. (2.3) the potentials are plotted for distances $r \leq r_c$, where $r_c^2 = 1/100\,\Lambda_{\overline{\mathrm{MS}}}^2$. For $\Lambda_{\overline{\mathrm{MS}}} = 0.1$ GeV, the "experimental" and the Coulombic potential overlap for distances 0.1 fm $\leq r \leq$ 0.2 fm, and they are clearly different in this region, as is obvious from Fig. 4. A quantitative measure of this discrepancy, which is independent of the absolute normalization of the potential, is the slope, integrated over the region under consideration, i.e., $\Delta V \equiv V(r = 0.2\ \mathrm{fm}) - V(r = 0.1\ \mathrm{fm})$. The potentials shown in Fig. 1 satisfy the inquality

$$\Delta V_{\min} \leq \Delta V \leq \Delta V_{\max},$$

$$\Delta V_{\min} = 458\ \mathrm{MeV}, \quad \Delta V_{\max} = 566\ \mathrm{MeV}.$$

The lower bound is given by the "softest" potential which is due to Martin[12] whereas the upper bound is inferred from the "Coulomb + linear" potential employed by the Cornell group.[15] The Coulombic QCD potential yields, for $\Lambda_{\overline{\mathrm{MS}}} = 0.1$ GeV,

$$\Delta V^{\mathrm{QCD}}(\Lambda_{\overline{\mathrm{MS}}} = 0.1\ \mathrm{GeV}) = 222\ \mathrm{MeV},$$

i.e., we have

$$\Delta V^{\mathrm{QCD}}(\Lambda_{\overline{\mathrm{MS}}} = 0.1\ \mathrm{GeV}) < \tfrac{1}{2}\Delta V_{\min}.$$

We therefore consider values of $\Lambda_{\overline{\mathrm{MS}}}$ less than or equal to 100 MeV to be highly unlikely. This lower bound is further supported by the fact that a potential, given by $V^{\mathrm{QCD}}(\Lambda_{\overline{\mathrm{MS}}} = 0.1\ \mathrm{GeV})$ for $r \leq 0.2$ fm and by the "experimental" one for $r > 0.2$ fm, leads to unacceptable results for the Υ spectroscopy which are shown in Table VIII.

For values of $\Lambda_{\overline{\mathrm{MS}}} \geq 0.2$ GeV, perturbation theory becomes unreliable before the potential overlaps with the experimentally known region

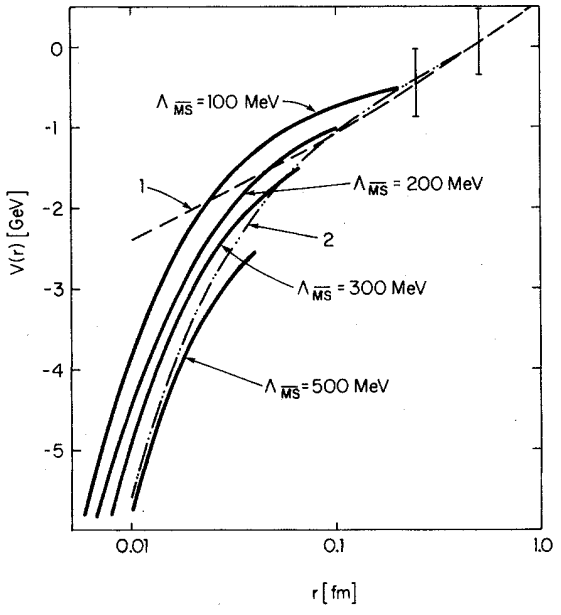

FIG. 4. Two-loop asymptotic-freedom potentials for four flavors and different values of $\Lambda_{\overline{\mathrm{MS}}}$ at distances $r \leq r_c$, $r_c^2 = 1/(100\Lambda_{\overline{\mathrm{MS}}}^2)$. For comparison the potentials (1) and (2) of Fig. 2 are also displayed. The "error bars" indicate the uncertainty with respect to absolute normalization.

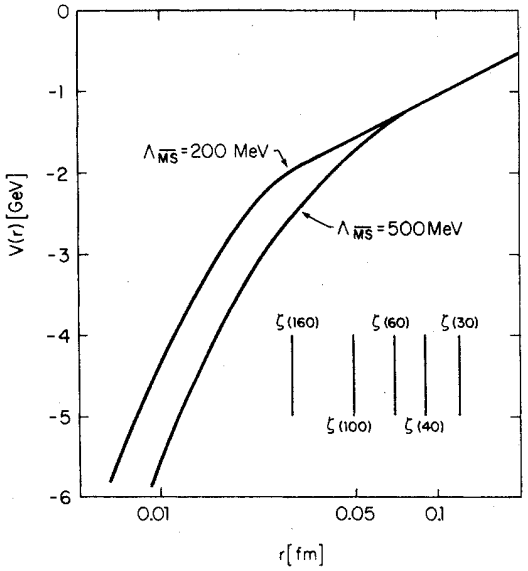

FIG. 5. Two $(Q\bar{Q})$ potentials which approach asymptotic-freedom potentials with $\Lambda_{\overline{\mathrm{MS}}} = 200$ MeV and $\Lambda_{\overline{\mathrm{MS}}} = 500$ MeV at short distances (see text). Mean-square radii of $(t\bar{t})$ ground states [denoted as $\zeta(2m_t)$] are shown for $\Lambda_{\overline{\mathrm{MS}}} = 500$ MeV and different quark masses m_t.

$r \geq 0.1$ fm. Therefore present quarkonia cannot distinguish between different values of $\Lambda_{\overline{\rm MS}}$ as long as they are larger than or equal to 200 MeV. In order to illustrate the sensitivity of heavier quarkonium spectroscopies on the scale parameter we have considered two potentials corresponding to $\Lambda_{\overline{\rm MS}} = 200$ MeV and $\Lambda_{\overline{\rm MS}} = 500$ MeV, which characterize a range of values compatible with the analysis of deep-inelastic scattering experiments.[39] The first potential (cf. Fig. 5) is obtained by extrapolating the "experimental" potential logarithmically below 0.1 fm until it intersects with the short-distance QCD potential; in the case $\Lambda_{\overline{\rm MS}} = 500$ MeV we use the potential of Sec. III. The results for the $1S$-$2S$ mass differences and the ground-state leptonic widths of a possible $(t\bar{t})$ system are displayed in Figs. 6 and 7 (for details, see Sec. V). They are compared with predictions obtained from the potential[12] $A + Br^{\nu}$, $\nu = 0.104$. It appears obvious that a toponium of mass $m(t\bar{t}) \geq 40$ GeV will be able to distinguish between power potentials and asymptotic freedom potentials as well as between different values of $\Lambda_{\overline{\rm MS}}$. We expect differences in the $1S$-$2S$ mass splittings between different potentials to be more than 70 MeV, and the leptonic widths will differ by more than 50%.

We therefore conclude that given the c- or b-quark mass, i.e., the absolute normalization of the potential, the $(t\bar{t})$ spectrum is very sensitive to Λ. The reason is simple: the $(t\bar{t})$ spectrum will determine the "experimental" potential down to distances of about 0.04 fm. Here the slopes of various asymptotic freedom potentials are quite similar; however, they differ substantially in their absolute normalization due to the different strength of the running coupling constant

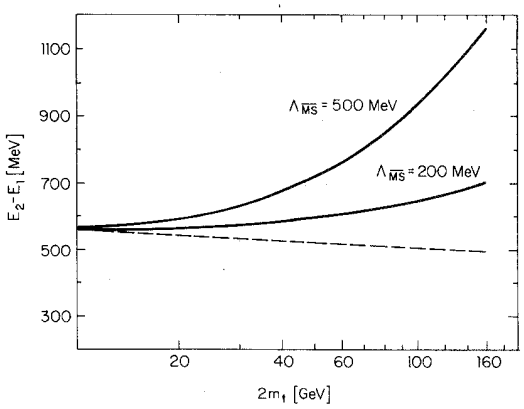

FIG. 6. $1S$-$2S$ mass differences as functions of t-quark mass m_t. The solid lines represent the potentials of Fig. 5, the dashed line Martin's potential (Ref. 12).

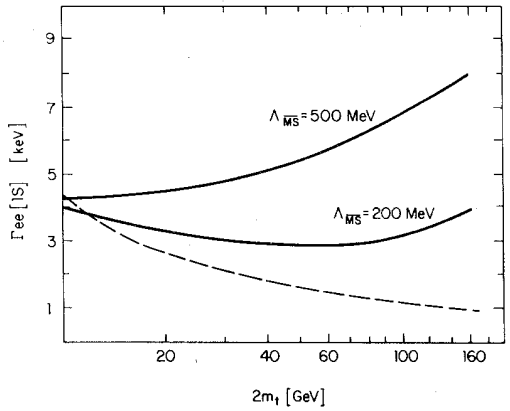

FIG. 7. Ground-state leptonic widths as a function of t-quark mass m_t. The solid lines correspond to the potentials of Fig. 5 and are based on Eq. (15) with a running coupling constant $\alpha_s(2m_t)$ inferred from Fig. 3. The dashed line shows the results of Martin's potential (Ref. 12). Here we have ignored weak-interaction effects, which would only enhance the differences (cf. Figs. 13, 14, and Sec. VI).

for different values of Λ (cf. Fig. 4). For instance, a change of $\Lambda_{\overline{\rm MS}}$ by 100 MeV changes the potential at 0.04 fm by about 300 MeV. Given the experimental potential down to 0.04 fm it can therefore distinguish different values of Λ. Unfortunately, the absolute normalization of the experimental potential is known only with an uncertainty of about ± 400 MeV which will lead to an uncertainty of ± 150 MeV in the determination of Λ.

A more precise determination of Λ may be possible by measuring hyperfine splittings[32] and electromagnetic and hadronic decay widths, where QCD corrections have recently been calculated by Barbieri, Curci, d'Emilio, and Remiddi[40] and Barbieri, Caffo, Gatto, and Remiddi.[41] At $m(t\bar{t}) = 60$ GeV, for instance, a change of $\Lambda_{\overline{\rm MS}}$ by 100 MeV will change the running coupling constant by ~7% (cf. Fig. 3) and consequently the total hadronic width by ~20%. A measurement of $\Gamma^{\rm had}(t\bar{t})$ with an accuracy of 20% would therefore determine the Λ parameter with an uncertainty of ± 100 MeV. This, in turn, would fix the normalization of the potential up to ± 300 MeV and thereby restrict the uncertainty of the quark masses to ± 150 MeV. Of course, these quantitative estimates must be used with caution, but we consider it an exciting possibility that the next quarkonium system might indeed provide the connection between the nonperturbative and the truly perturbative regimes and in this way determine the entire $(Q\bar{Q})$ potential as well as the Λ parameter in QCD.

TABLE IX. Properties of $(t\bar{t})$ spectra: S states (potential with $\Lambda_{\overline{\rm MS}} = 200$ MeV, for comparison).

m_t (GeV)	$-E_B$ (MeV)	$E_2 - E_1$ (MeV)	$E_3 - E_1$ (MeV)	$E_4 - E_1$ (MeV)	$(E_3 - E_2)/(E_2 - E_1)$
15	693	572	874	1094	0.528
20	807	587	887	1101	0.511
25	898	600	901	1112	0.502
30	974	610	913	1123	0.497
40	1101	629	939	1148	0.493
50	1207	645	964	1175	0.495
60	1330	661	990	1203	0.498
70	1386	679	1017	1234	0.498
80	1466	698	1046	1266	0.499

V. HEAVIER QUARKONIUM SPECTROSCOPIES

In this section some properties of heavier quarkonium spectra are listed for t-quark masses in the range 15 GeV $\leq m_t \leq$ 80 GeV. The calculations have been carried out for the two $(Q\bar{Q})$ potentials (shown in Fig. 5) which at short distances approach Coulomb-type QCD potentials characterized by scale parameters $\Lambda_{\overline{\rm MS}} = 200$ MeV and $\Lambda_{\overline{\rm MS}} = 500$ MeV, respectively.

We have computed the ground-state binding energies (E_B, Tables IX and XII), the excitation energies for the first three S states ($E_n - E_1$, Tables IX and XII), the first two P states ($E_{nP} - E_{1S}$, Tables X and XIII) and the first two D states ($E_{nD} - E_{1S}$, Tables X and XIII). We also listed the ratios $(E_3 - E_1)/(E_2 - E_1)$ (Tables IX and XII) and $(E_{2S} - E_{1P})/(E_{2S} - E_{1S})$ (Tables X and XIII) which are most sensitive to the effective power[10] characterizing the potential at distances of the corresponding mean-square radii. The leptonic widths of the ground states have been evaluated with $[\Gamma_{ee}(1S)$, cf. Eq. (3.2)] and without $[\Gamma_{ee}^{(0)}(1S)$, cf. Eq. (3.1)] radiative corrections [the value of $\alpha_s(2m_t)$ can be read off from Fig. 3]; in addition the ratios of leptonic widths $[\Gamma_{ee}(nS)/\Gamma_{ee}(1S)]$, the velocities $(\langle v^2/c^2\rangle_{1S})$ and the mean-square radii $(\langle r^2\rangle_{1S}^{1/2})$ of the ground states are listed (Tables XI and XIV).

Figure 8 shows the binding energies of the first four S states and the two lowest P and D states. In Fig. 9 we have plotted all S states below continuum threshold as a function of the t-quark mass. Following standard methods[10,33] we have estimated the continuum threshold (CT) at

$$E_{\rm CT} = 2m_t + 0.91 \text{ GeV}. \tag{5.1}$$

The number of S states encountered below continuum threshold agrees with the semiclassical estimate of Quigg and Rosner,[42]

$$n \approx 2\left(\frac{m_t}{m_c}\right)^{1/2}. \tag{5.2}$$

The mean-square radii of the ground states are displayed in Fig. 5, indicating the distances down to which the $(Q\bar{Q})$ potential is probed by toponium systems of various masses.

The effect of logarithmic corrections to the Coulomb part of the $(Q\bar{Q})$ potential and their importance with respect to $(t\bar{t})$ spectra has previously been investigated by Krasemann and Ono[43]

TABLE X. Properties of $(t\bar{t})$ spectra: P and D states (potential with $\Lambda_{\overline{\rm MS}} = 200$ MeV, for comparison).

m_t (GeV)	$E_{1P} - E_{1S}$ (MeV)	$E_{2P} - E_{1S}$ (MeV)	$E_{1D} - E_{1S}$ (MeV)	$E_{2D} - E_{1S}$ (MeV)	$(E_{2S} - E_{1P})/(E_{2S} - E_{1S})$
15	446	784	700	950	0.22
20	459	801	719	964	0.218
25	470	816	734	979	0.217
30	480	831	748	993	0.213
40	500	860	774	1023	0.205
50	521	890	800	1054	0.192
60	545	920	827	1085	0.180
70	572	951	856	1118	0.158
80	600	983	885	1152	0.140

TABLE XI. Properties of $(t\bar{t})$ spectra: leptonic widths, velocities, and mean-square radii. The leptonic widths do not include weak-interaction effects (potential with $\Lambda_{\overline{\rm MS}} = 200$ MeV, for comparison).

m_t (GeV)	$\Gamma_{ee}(1S)$ (keV)	$\Gamma_{ee}^{(0)}(1S)$ (keV)	$\Gamma_{ee}(2S)/\Gamma_{ee}(1S)$	$\Gamma_{ee}(3S)/\Gamma_{ee}(1S)$	$\Gamma_{ee}(4S)/\Gamma_{ee}(1S)$	$\langle v^2/c^2\rangle_{1S}$	$\langle r^2\rangle^{1/2}_{1S}$ (fm)
15	3.00	3.77	0.43	0.29	0.24	0.026	0.13
20	2.85	3.58	0.43	0.29	0.23	0.020	0.11
25	2.85	3.50	0.43	0.28	0.22	0.017	0.10
30	2.83	3.48	0.43	0.28	0.21	0.014	0.09
40	2.91	3.58	0.44	0.27	0.20	0.011	0.07
50	3.13	3.77	0.435	0.26	0.19	0.010	0.06
60	3.35	4.04	0.42	0.24	0.17	0.009	0.06
70	3.61	4.35	0.40	0.23	0.16	0.008	0.05
80	3.90	4.70	0.38	0.21	0.15	0.008	0.05

TABLE XII. Properties of $(t\bar{t})$ spectra: S states (potential of Ref. 13, $\Lambda_{\overline{\rm MS}} = 500$ MeV).

m_t (GeV)	$-E_B$ (MeV)	E_2-E_1 (MeV)	E_3-E_1 (MeV)	E_4-E_1 (MeV)	$(E_3-E_2)/(E_2-E_1)$
15	778	629	941	1166	0.496
20	932	674	989	1209	0.467
25	1064	718	1040	1258	0.448
30	1182	762	1090	1309	0.430
40	1390	847	1191	1411	0.406
50	1572	929	1288	1512	0.386
60	1738	1006	1381	1610	0.373
70	1892	1082	1472	1706	0.360
80	2036	1154	1560	1799	0.352

TABLE XIII. Properties of $(t\bar{t})$ spectra: P and D states (potential of Ref. 13, $\Lambda_{\overline{\rm MS}} = 500$ MeV).

m_t (GeV)	$E_{1P}-E_{1S}$ (MeV)	$E_{2P}-E_{1S}$ (MeV)	$E_{1D}-E_{1S}$ (MeV)	$E_{2D}-E_{1S}$ (MeV)	$(E_{2S}-E_{1P})/(E_{2S}-E_{1S})$
15	528	866	786	1035	0.161
20	576	920	843	1089	0.145
25	623	973	900	1144	0.132
30	668	1026	955	1200	0.123
40	754	1129	1060	1308	0.110
50	835	1227	1160	1412	0.101
60	911	1321	1255	1514	0.094
70	984	1411	1347	1612	0.090
80	1054	1500	1435	1706	0.087

TABLE XIV. Properties of $(t\bar{t})$ spectra: leptonic widths, velocities, and mean-square radii. The leptonic widths do not include weak-interaction effects (potential of Ref. 13, $\Lambda_{\overline{\rm MS}} = 500$ MeV).

m_t (GeV)	$\Gamma_{ee}(1S)$ (keV)	$\Gamma_{ee}^{(0)}(1S)$ (keV)	$\Gamma_{ee}(2S)/\Gamma_{ee}(1S)$	$\Gamma_{ee}(3S)/\Gamma_{ee}(1S)$	$\Gamma_{ee}(4S)/(\Gamma_{ee}(1S)$	$\langle v^2/c^2\rangle_{1S}$	$\langle r^2\rangle^{1/2}_{1S}$ (fm)
15	4.79	6.43	0.35	0.23	0.18	0.034	0.12
20	5.10	6.69	0.33	0.21	0.16	0.028	0.09
25	5.33	6.99	0.31	0.19	0.14	0.025	0.08
30	5.68	7.29	0.30	0.18	0.13	0.022	0.07
40	6.26	7.86	0.28	0.16	0.11	0.019	0.06
50	6.69	8.41	0.26	0.14	0.10	0.017	0.05
60	7.14	8.93	0.25	0.14	0.09	0.016	0.04
70	7.54	9.43	0.24	0.13	0.09	0.015	0.04
80	7.92	9.90	0.24	0.12	0.08	0.014	0.03

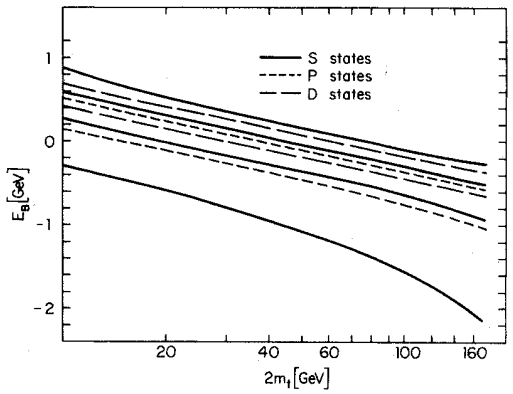

FIG. 8. Binding energies of lowest-lying S, P, and D states of a $(t\bar{t})$ system as function of the t-quark mass m_t ($\Lambda_{\overline{\rm MS}}$ =500 MeV).

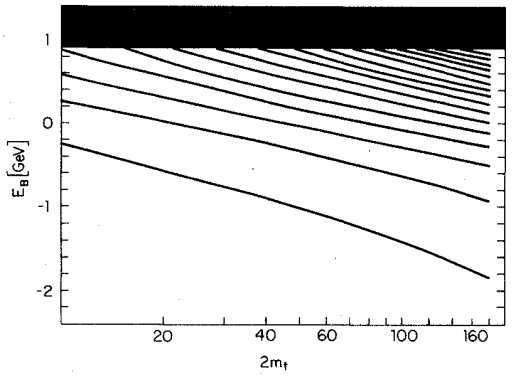

FIG. 9. $(t\bar{t})$ S-wave bound states below threshold as function of the t-quark mass. The binding energies have been computed for a potential which corresponds to $\Lambda_{\overline{\rm MS}}$ =300 MeV; it satisfies $V(\Lambda_{\overline{\rm MS}}$ =200 MeV) $\geq V(\Lambda_{\overline{\rm MS}}$ =300 MeV) $\geq V(\Lambda_{\overline{\rm MS}}$ =500 MeV).

and Krammer, Krasemann, and Ono.[44] Reference 43 contains also a discussion of the fine and hyperfine structure of $(t\bar{t})$ spectroscopies, based on the Breit-Fermi Hamiltonian.

In Table XV some properties of a $(t\bar{t})$ system with m_t =20 GeV and m_t =30 GeV are compared for $\Lambda_{\overline{\rm MS}}$ =0.2 GeV, $\Lambda_{\overline{\rm MS}}$ =0.5 GeV, and Richardson's potential. As m_t increases, the differences between these models also increase. The predictions of the three models are clearly distinguishable experimentally. This illustrates once more that a $(t\bar{t})$ system will lead to quantitative tests of QCD as well as the determination of the scale parameter Λ.

It is a straightforward exercise to evaluate $(t\bar{c})$ and $(t\bar{b})$ mass spectra. Their ground-state masses are given by

$$M(t\bar{c}) = m_t + m_c + E_B(t\bar{c}),$$
$$M(t\bar{b}) = m_t + m_b + E_B(t\bar{b}), \tag{5.3}$$

where m_c=1.48 GeV and m_b=4.88 GeV. The binding energies $E_B(t\bar{c})$ and $E_B(t\bar{b})$ as well as the square of the wave functions at the origin are plotted in Figs. 10 and 11 as functions of the corresponding reduced masses $m_R(t\bar{c})$ and $m_R(t\bar{b})$.

Figure 12 displays the S-wave binding energies E_B of various quarkonium systems as a function of the corresponding mean-square radii $\langle r^2\rangle^{1/2}$. Obviously, the following relation holds approximately,

$$E_B \approx V(\langle r^2\rangle^{1/2}), \tag{5.4}$$

independent of the quark mass and the principal quantum number of the S-state under consideration. This is not unexpected as power-law potentials of the form $V=\lambda r^{\epsilon}$ imply[10]

$$E_B = \left\langle \frac{1}{2} r \frac{dV}{dr} \right\rangle + \langle V\rangle = \left(1+\frac{\epsilon}{2}\right)\langle V\rangle \tag{5.5}$$

and smoothly varying potentials satisfy $\langle V(r)\rangle$

TABLE XV. Comparison of $(t\bar{t})$ spectra for different QCD-like potential models.

m_t=20 GeV	$\Lambda_{\overline{\rm MS}}$ = 0.2 GeV	$\Lambda_{\overline{\rm MS}}$ = 0.5 GeV	Richardson (N_f=3)
$-E_B$ (MeV)	807	932	975
E_2-E_1 (MeV)	587	674	700
E_3-E_1 (MeV)	887	989	1017
$\Gamma_{ee}(2S)/\Gamma_{ee}(1S)$	0.43	0.33	0.31
$\Gamma_{ee}(3S)/\Gamma_{ee}(1S)$	0.29	0.21	0.19
m_t=30 GeV			
$-E_B$ (MeV)	974	1182	1240
E_2-E_1 (MeV)	610	762	801
E_3-E_1 (MeV)	913	1090	1136
$\Gamma_{ee}(2S)/\Gamma_{ee}(1S)$	0.43	0.30	0.29
$\Gamma_{ee}(3S)/\Gamma_{ee}(1S)$	0.28	0.18	0.17

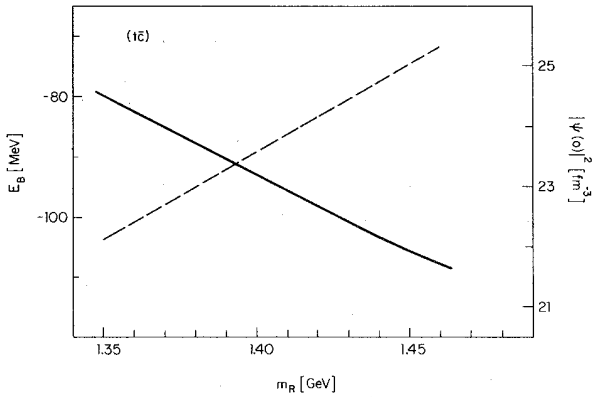

FIG. 10. Binding energy (solid line) and wave function squared at the origin (dashed line) of the lowest $(t\bar{c})$ bound state as functions of $m_R \equiv m_c m_t/(m_c+m_t)$ ($\Lambda_{\overline{\rm MS}}$ =500 MeV).

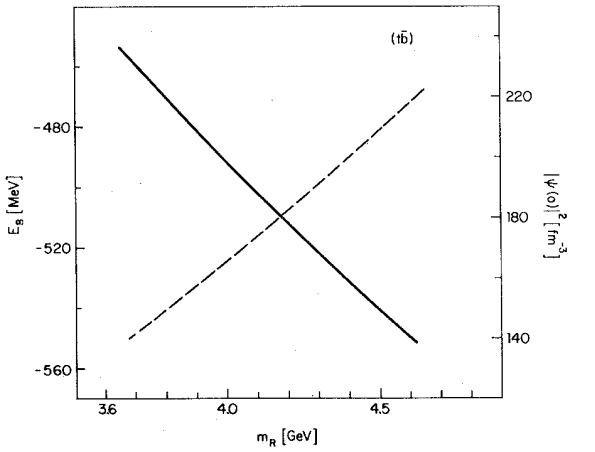

FIG. 11. Binding energy (solid line) and wave function squared at the origin (dashed line) of the lowest $(t\bar{b})$ bound state as functions of $m_R \equiv m_b m_t/(m_b+m_t)$ ($\Lambda_{\overline{\rm MS}}$ =500 MeV).

$\approx V(\langle r^2\rangle^{1/2})$. Equation (5.4) provides a useful guide to estimate the relation between binding energy and size of the quarkonium system under consideration.

VI. Z-BOSON EFFECT

So far, we have neglected weak-interaction effects. The leptonic widths quoted are actually leptonic widths due to the electromagnetic interaction: $(Q\bar{Q})\to\gamma^*\to l^-l^+$. For ψ and Υ families, the contribution due to the Z boson is negligible. However, for the t quark, the Z-boson-mediated decay is important. This has been discussed in the literature.[45] For $\zeta(Q\bar{Q})\to f\bar{f}$, the lowest-order electromagnetic and weak decay widths are given by (in familiar notation)

$$\Gamma(\zeta\to\gamma^*, Z^*\to f\bar{f}) = \frac{4\pi\alpha^2}{m_\zeta{}^2}\,4e_Q{}^2|\psi(0)|^2\sum_f\left\{e_f{}^2+\frac{2e_f}{e_Q}\,\frac{v_Q v_f(m_\zeta{}^2-m_Z{}^2)m_\zeta{}^2}{[(m_\zeta{}^2-m_Z{}^2)^2+m_Z{}^2\Gamma_Z{}^2](2\sin 2\theta_W)^2}\right.$$
$$\left.+\frac{v_Q{}^2(v_f{}^2+a_f{}^2)m_\zeta{}^4}{e_Q{}^2[(m_\zeta{}^2-m_Z{}^2)^2+m_Z{}^2\Gamma_Z{}^2](2\sin 2\theta_W)^4}\right\}, \tag{6.1}$$

where the sum is over all fermions (quarks are to be counted three times due to color); the standard model implies

$$\begin{aligned} v_e &= v_\mu = v_\tau = -1+4\sin^2\theta_W,\\ a_e &= a_\mu = a_\tau = -1,\\ a_\nu &= v_\nu = 1,\\ v_u &= v_c = v_t = 1-\tfrac{8}{3}\sin^2\theta_W,\\ a_u &= a_c = a_t = 1,\\ v_d &= v_s = v_b = -1+\tfrac{4}{3}\sin^2\theta_W,\\ a_d &= a_s = a_b = -1. \end{aligned} \tag{6.2}$$

To obtain some idea of the magnitude of the width, let us consider $\Gamma(\zeta\to\gamma^*, Z^*\to\text{all})$,[46] taking Γ_Z =3 GeV, $\sin^2\theta_W$ =0.23,[47] and m_Z =89 GeV. Clearly the Z-boson effect becomes dominant as $m_\zeta\to m_Z$. This is displayed in Fig. 13. For

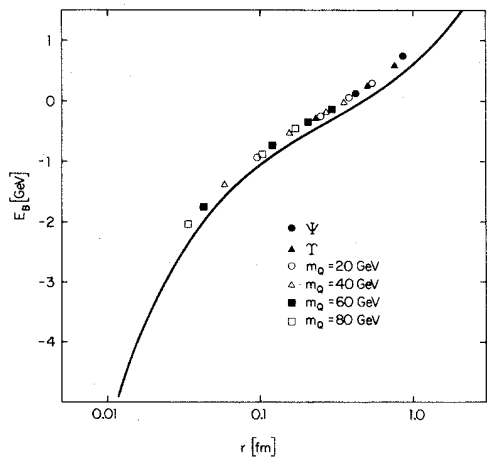

FIG. 12. Binding energies of the S states versus the corresponding mean-square radii for various quark masses, compared to the $(Q\bar{Q})$ potential ($\Lambda_{\overline{\rm MS}}$ =500 MeV).

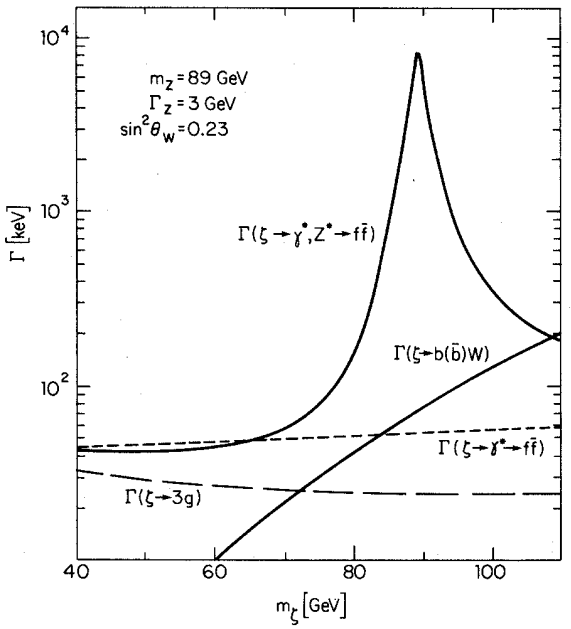

FIG. 13. Z-boson effect. Electromagnetic, electroweak, and hadronic decay widths as functions of the $(t\bar{t})$ mass m_ζ. $\Gamma(\zeta\to b(\bar{b})W)$ denotes the partial width due to the weak decay of the t $(\bar{t})$ quark; for a detailed discussion, see Kühn (Ref. 45).

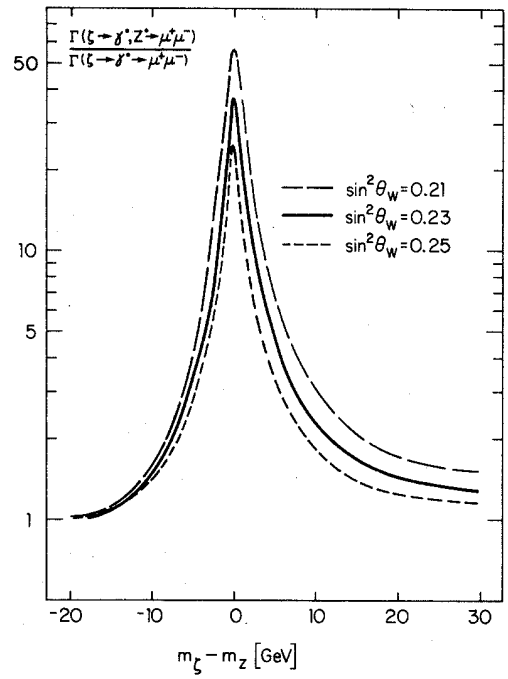

FIG. 14. Ratio of total and electromagnetic leptonic widths for different values of the Weinberg angle θ_W.

comparison, we have included $\Gamma(\zeta\to\gamma^*\to\text{all})$ and $\Gamma(\zeta\to\text{three gluons}\to\text{hadrons})$.

The three-gluon decay mode is estimated from the Υ decay using the lowest-order formula. Using the data available,[35] we obtain $\alpha_s(m(\Upsilon))=0.20$ and $\Lambda_{3g}=0.240$ GeV. (Of course, the relation between Λ_{3g} and $\Lambda_{\overline{\text{MS}}}$ is determined by the α_s correction to this process.)[48,49] It is intriguing to note that for $m_\zeta>70$ GeV, the weak interaction dominates in the ζ decay width followed by the electromagnetic interaction while the strong interation provides the weakest contribution to ζ decay.

This remarkable phenomenon, namely the reversal of the strengths of the strong, electromagnetic, and weak interactions, persists even for $m_\zeta \gtrsim m_Z$. The leptonic widths of ζ and its S-wave excited states increase as the mass of the states approach that of the Z mass. In Fig. 14, we have plotted the ratio

$$r_{l^+l^-}=\frac{\Gamma(\zeta\to\gamma^*,Z^*\to l^+l^-)}{\Gamma(\zeta\to\gamma^*\to l^+l^-)} \tag{6.3}$$

for different values of the Weinberg angle. The signal of the resonance peak is proportional to the leptonic width,

$$\int\sigma(e^+e^-\to\zeta\to f\bar{f})dE\sim\frac{6\pi^2}{m_\zeta{}^2}\frac{\Gamma_{ee}\Gamma_f}{\Gamma} \tag{6.4}$$

or

$$\int R\,dE\sim\frac{9\pi}{2\alpha^2}\Gamma_{ee}. \tag{6.5}$$

For a given energy spread δE, the resonance signal would have a peak value of

$$R_{\text{peak}}=\frac{\int R\,dE}{\sqrt{2\pi}\delta E}. \tag{6.6}$$

As an illustration, if $\delta E=100\text{ MeV}\times(E/100\text{ GeV})^2$, we have

$$R_{\text{peak}}=1.06\left(\frac{100\text{ GeV}}{m_\zeta}\right)^2\Gamma(\zeta\to\gamma^*,Z^*\to e^+e^-,\text{ in keV}) \tag{6.7}$$

where ζ can be any of the S-wave bound states. R_{peak} as well as the nonresonant contribution to R, which is strongly affected by the Z pole, are displayed in Fig. 15. Both the resonance peak signal and the background are greatly enhanced by the presence of the Z pole. This should help the search for heavy quarkonium states in the vicinity of the Z pole, where—due to high statistics—even a small signal to background ratio may be observable.

Around the Z mass, the energy difference between the ζ ground state and its highest excited state below the continuum threshold is of the

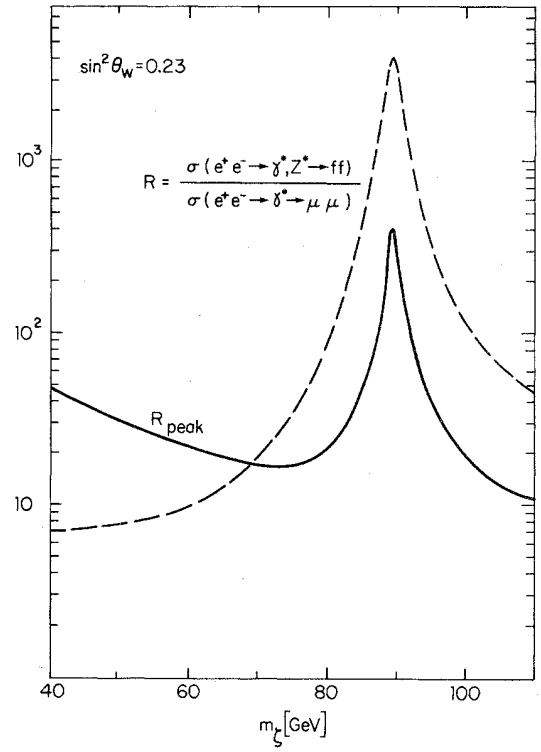

FIG. 15. The value of R as a function of energy, $R_{\text{peak}} = \sigma(e^+e^- \to \zeta \to \gamma^*, Z^* \to f\bar{f})/\sigma(e^+e^- \to \gamma^* \to \mu^+\mu^-)$, where the beam spread [cf. Eq. (6.7)] has been included.

order of 2 GeV. For $m_Z \gtrsim m_\zeta$, the leptonic widths of the higher excited states would have more contributions from the Z boson than that of the lower excited states. Hence we can even envision the situation where the resonance peak of a higher excited state is bigger than that of a lower state. In fact, if $m_\zeta \sim m_Z$, a whole array of new exciting phenomena can be expected.

VII. SUMMARY AND DISCUSSION

In the preceding sections we have reexamined the evidence which quarkonium spectroscopies provide for quantum chromodynamics. So far a theory of mesons and baryons, which would allow a systematic computation of their mass spectra, has not been derived from the fundamental interaction of quarks and gluons. Therefore we had to start from a set of theoretical expectations, based on QCD, which appear to be generally accepted: the nonrelativistic nature of heavy-quark bound states, the flavor independence of the binding force, and the asymptotic behavior of the potential at large and small distances as dictated by linear confinement and asymptotic freedom.

It was shown that a potential model, based on this set of assumptions, yields an accurate description of both the ψ and Υ families. Furthermore, the parameters characterizing the large- and small-distance behavior, i.e., the Regge slope α' and the QCD scale parameter Λ, are in quantitative agreement with values measured in light-hadron spectroscopy and deep-inelastic scattering experiments; we obtain $\alpha' = 1\ \text{GeV}^{-2}$ and $\Lambda_{\overline{\text{MS}}} = 500$ MeV [given the β function Eq. (2.12), the sensitivity of the Υ spectrum with respect to Λ can be seen by comparing models 2 and 2a in Table VIII]. We also find that the absolute values of the leptonic widths and the ψ-η_c hyperfine splitting are in agreement with experiment. As these quantities are particularly sensitive to the short-distance behavior of the $(Q\bar{Q})$ potential, this agreement strongly supports the idea of asymptotic freedom. The only failure of the potential model appears to be the $E1$ transitions, where the discrepancies between our predictions and the measured rates amount to a factor 2 to 4. However, as the emitted photons carry momenta of only a few hundred MEV, we expect large QCD corrections to the lowest-order transition amplitudes. Within our present theoretical understanding of the $E1$ transitions we do not consider the discrepancy between experiment and zeroth-order theory to be very worrisome.

Unfortunately, our lack of understanding concerning the $E1$ transitions as well as the fine structure of charmonium does not allow us to determine the c- and b-quark masses accurately. Potential models employ c-quark masses ranging from 1.1 GeV to 1.9 GeV. In addition, there are uncertainties in the theoretical predictions for leptonic widths because of unknown relativistic and higher-order radiative corrections. These theoretical ambiguities as well as experimental uncertainties prohibit a clear distinction between QCD-like models and the logarithmic or small-power potentials on the basis of present experimental data. Only a heavier quarkonium system will settle this issue.

It is interesting, however, that the ψ and Υ families contain already quantitative information on the Λ parameter, if we accept that the short-distance behavior of the $(Q\bar{Q})$ potential is governed by asymptotic freedom. For small values of Λ, i.e., small values of α_s, one expects a Coulombic potential up to large distances. Therefore the "experimental" potential, which has been measured down to 0.1 fm, provides a lower bound for Λ. Our investigations lead to $\Lambda_{\overline{\text{MS}}} > 100$ MeV.

The analysis of deep-inelastic scattering ex-

periments suggests values of $\Lambda_{\overline{\rm MS}}$ between 0.2 and 0.5 GeV.[39] Our calculations of $(t\bar{t})$ spectra demonstrate that the next quarkonium system will allow a distinction not only between QCD-like and small-power potentials, but also between different Λ parameters. This would be most valuable since the determination of Λ from deep-inelastic scattering processes is plagued with ambiguities due to unknown higher-twist effects. The $(t\bar{t})$ family will measure the $(Q\bar{Q})$ potential down to distances of about 0.04 fm. If the value of $\Lambda_{\overline{\rm MS}}$ ranges indeed between 200 and 500 MeV, the $(t\bar{t})$ spectrum will provide the connection between the perturbative and the nonperturbative regimes and in this way determine the entire $(Q\bar{Q})$ potential.

We have dealt mainly with the evidence for asymptotic freedom which can be inferred from quarkonia. The evidence for linear[50] confinement appears—at least at this moment—to be weaker. Thus, at present any determination of the Regge slope, based on quarkonia, can only be consistent with experiment. The $(t\bar{t})$ spectrum will contain many excited states with mean-square radii between 0.5 and 1.0 fm. An accurate determination of the $(Q\bar{Q})$ potential may lead to a clear identification of the expected linear asymptotic behavior. At distances larger than 1.0 fm, however, the simple potential picture breaks down due to threshold effects, and the existence of light quarks seems to demand a relativistic, field-theoretic treatment.

An important question which remains to be investigated in detail is the influence of nonperturbative effects[26,27,51-53] on the short-distance part of the $(Q\bar{Q})$ potential. In principle, the potential proposed in Ref. 13 has included both the perturbative and the nonperturbative effects (phenomenologically, of course) for all distances. However, it is still interesting to estimate the nonperturbative effects from a theoretical point of view. For example, let us consider gluonic vacuum fluctuations, characterized by a nonvanishing expectation value $\phi \equiv \langle 0|(\alpha_s/\pi)G_{\mu\nu}G_{\mu\nu}|0\rangle$. A simple dimensional analysis suggests that the effect of ϕ on the potential is negligible for distances less than 0.1 fm, which are relevant for our discussion of the perturbative part of the potential. With $\phi = 0.012$ GeV^4,[51] we obtain $\delta V(r) \equiv \phi r^3 < 2$ MeV, a correction of about 0.2% to the perturbative Coulomb-type potential.

We have only briefly discussed weak-interaction effects.[45] These are of great importance if the $(t\bar{t})$ mass is close to the Z-boson mass; in this case a variety of new phenomena can be expected.

Besides measuring the quark-antiquark force, heavy quarkonia may also exhibit additional states not expected on the basis of a potential model. Such "vibrational states"[54] are expected as a result of coherent gluonic excitations and have been investigated on the basis of string models. The existence of these states would provide further evidence for additional gluonic degrees of freedom.

In conclusion, the theoretical expectations based on QCD lead to a potential model for quarkonia which is in excellent agreement with experiment. The $(Q\bar{Q})$ potential has emerged as a conceptually simple, experimentally well-measurable quantity, which allows a comparison with QCD at all coupling strengths.[27,55] Further theoretical work on fine-structure, electromagnetic and hadronic transitions and decays, and (it is hoped) the discovery of a new quarkonium system will provide stringent quantitative tests of the fundamental theory of strong interactions.

ACKNOWLEDGMENTS

This work is an extension of earlier work in collaboration with G. Grunberg. We thank him for numerous discussions. We have also benefitted from discussions with our colleagues at Cornell and Fermilab, especially W. Bardeen, K. Gottfried, Y. P. Kuang, P. Lepage, C. Quigg, J. Rosner, T. M. Yan, and D. Yennie. One of us (W.B.) acknowledges the kind hospitality of the theory groups at Cornell University and the Fermi National Accelerator Laboratory.

APPENDIX A

The potential, used in Sec. III, is defined in terms of the β function Eq. (2.12) (with $l = 24$), the relation Eq. (2.8a), and Eq. (2.4). In order to obtain $V(Q^2)$ one first has to carry out the integration in Eq. (2.8a), yielding

$$\ln\frac{Q^2}{\Lambda^2} = \ln(e^{1/b_0\rho} - 1) + \frac{b_1}{b_0^2}\left(\ln\frac{b_0}{l} - \gamma_E - E_1(l\rho)\right), \tag{A1}$$

where $\gamma_E = 0.5772\ldots$ is Euler's constant and $E_1(x)$ the exponential integral.[56] We do not know how to invert Eq. (A1) analytically; a very good approximation, however, is given by

$$\hat{\rho}(Q^2) = \frac{1}{b_0 \ln[1 + \eta(Q^2)(Q^2/\Lambda^2)]}, \tag{A2a}$$

where

$$\eta(Q^2) = \left(\frac{l}{b_0}\right)^{b_1/b_0^2} \exp\left(\frac{b_1}{b_0^2}[\gamma_E + E_1(l\rho_0(Q^2))]\right) \tag{A2b}$$

and

$$\rho_0(Q^2) = \frac{1}{b_0 \ln\left(1 + \frac{Q^2}{\Lambda^2}\right)} . \qquad \text{(A2c)}$$

It is easy to check that $\rho(Q^2)$, as given by Eq. (A2), has the correct asymptotic behaviors,

$$\hat{\rho}(Q^2) \underset{Q^2 \to 0}{\sim} \frac{K}{Q^2} , \qquad \text{(A3a)}$$

$$K = \frac{\Lambda^2}{b_0} \exp\left[- \frac{b_1}{b_0^2} \left(\gamma_E + \ln \frac{l}{b_0} \right) \right] ,$$

and

$$\hat{\rho}(Q^2) \underset{Q^2 \to \infty}{\sim} \frac{1}{b_0 \ln(Q^2/\Lambda^2)} - \frac{b_1}{b_0^3} \frac{\ln\ln(Q^2/\Lambda^2)}{\ln^2(Q^2/\Lambda^2)} + O\left(\frac{1}{\ln^3(Q^2/\Lambda^2)} \right) . \qquad \text{(A3b)}$$

Equation (A3a), together with Eqs. (2.9) and (2.10), leads to the relation Eq. (2.13) between Regge slope α' and scale parameter $\Lambda_{\overline{\rm MS}}$. A numerical comparison shows that at intermediate values of Q^2, $\hat{\rho}(Q^2)$ approximates $\rho(Q^2)$ with an error of less than 1%.

The potential in coordinate space is given by

$$\tilde{V}(\vec{r}) = -16\pi^2 C_2(R) \int \frac{d^3q}{(2\pi)^3} \frac{\hat{\rho}(q^2)}{q^2} e^{i\vec{q}\cdot\vec{r}} \qquad \text{(A4)}$$

and may be conveniently written as[57]

$$\tilde{V}(r) = kr - \frac{2\pi C_2(R)}{b_0} \frac{v(\lambda r)}{r} , \qquad \text{(A5a)}$$

where

$$k = \frac{1}{2\pi\alpha'} \qquad \text{(A5b)}$$

and

$$v(x) = \frac{4b_0}{\pi} \int_0^\infty \frac{dQ}{Q} \left(\hat{\rho}(Q^2) - \frac{K}{Q^2} \right) \sin\left(\frac{Q}{\lambda} x \right) . \qquad \text{(A5c)}$$

The parameter λ can be expressed in terms of the string constant k or the scale parameter $\Lambda_{\overline{\rm MS}}$,

$$\lambda = \left(\frac{b_0 k}{2\pi C_2(R)} \right)^{1/2} \qquad \text{(A5d)}$$

and

$$\lambda = \Lambda_{\overline{\rm MS}} \exp\left\{ \frac{1}{2b_0} \left[\tfrac{31}{9} C_2(G) - \tfrac{10}{9} N_f \right] - \frac{b_1}{2b_0^2} \left(\gamma_E + \ln \frac{l}{b_0} \right) \right\} , \quad l = 24 . \qquad \text{(A5e)}$$

$v(x)$ varies slowly with x, and for our numerical calculations we have used a linear interpolation between 26 points which are listed in Table XVI.

For $\alpha' \sim 1$ GeV^{-2}, one obtains $\lambda \sim 400$ MeV, i.e., the smallest nonzero x value in Table XVI, $x_1 = 0.01$, corresponds to a distance $r_1 \sim 0.005$ fm. At such short distances $\tilde{V}(r)$ has already approached the Coulombic potential for $\Lambda_{\overline{\rm MS}} = 0.5$ GeV, which we then use to extrapolate $\tilde{V}(r)$ to even shorter distances, assuming $N_f = 4$. The entire potential is finally given by

$$\tilde{V}(r) = kr - \frac{8\pi}{27} \frac{v(\lambda r)}{r} , \quad r \geq 0.01 \text{ fm}$$

and

$$\tilde{V}(r) = -\frac{16\pi}{25} \frac{1}{r \ln(1/\Lambda_{\overline{\rm MS}}{}^2 r^2)} \left[1 + (2\gamma_E + \tfrac{53}{75}) \frac{1}{\ln(1/\Lambda_{\overline{\rm MS}}{}^2 r^2)} - \frac{462}{625} \frac{\ln\ln(1/\Lambda_{\overline{\rm MS}}{}^2 r^2)}{\ln(1/\Lambda_{\overline{\rm MS}}{}^2 r^2)} \right] , \quad r < 0.01 \text{ fm} \qquad \text{(A6)}$$

with $\Lambda_{\overline{\rm MS}} = 0.509$ GeV, $k = 0.153$ GeV^2, $\alpha' = 1.04$ GeV^{-2}, $\lambda = 0.406$ GeV, $\gamma_E = 0.5772\ldots$, and $v(x)$ as given in Table XVI.

TABLE XVI. Numerical values of the dimensionless function $v(x)$ characterizing the QCD-type potential of Ref. 13 [cf. Appendix A, Eqs. (A.5)].

x_n	v_n	x_n	v_n	x_n	v_n
0	0	0.40	0.766	1.30	0.953
0.01	0.249	0.50	0.811	1.40	0.960
0.02	0.300	0.60	0.845	1.50	0.965
0.03	0.339	0.70	0.872	1.60	0.970
0.04	0.370	0.80	0.893	1.70	0.974
0.05	0.397	0.90	0.911	1.80	0.977
0.10	0.499	1.00	0.925	1.90	0.980
0.20	0.624	1.10	0.936	2.00	0.982
0.30	0.707	1.20	0.946		

APPENDIX B

Recently the question of relativistic and radiative corrections[58] to the leptonic widths of heavy quarkonia has been investigated and different conclusions have been drawn concerning their importance. It seems to us that Eq. (3.2) is a reliable estimate of radiative corrections. We believe, however, that a consistent evaluation of all v^2/c^2 corrections is a hopeless task before a much deeper understanding of bound states in the framework of QCD has been achieved. In

order to substantiate this opinion and to obtain a clear picture of where various uncertainties may arise, we will briefly review how Eq. (3.2) arises in the framework of the Bethe-Salpeter (BS) formalism for relativistic bound states.

Let us assume that the $(Q\bar{Q})$ system can be described by a Green's function $G(W,p,q)$ which has poles at bound-state energies $M_n(Q\bar{Q})=2W_n$,

$$G(W,p,q)\sim\frac{\psi(W_n,p)\bar{\psi}(W_n,q)}{W-W_n-i\epsilon}\,,\quad W\sim W_n\,. \tag{B1}$$

For simplicity, we consider the quarkonium system in its c.m. system, i.e., the total four-momentum is given by $P_n^\mu=(2W_n,\vec{0})$; p and q denote the relative four-momenta in initial and final state and $\psi(W_n,p)$ is the BS wave function. The Green's function satisfies the BS equation

$$G(W,p,q)=(2\pi)^4\delta^4(p-q)G_F(W,p)+G_F(W,p)\int\frac{d^4q'}{(2\pi)^4}\,K(W,p,q')G(W,q',q), \tag{B2}$$

where $G_F(W,p)\equiv iS^{(1)}(\frac{1}{2}P+p)iS^{(2)}(-\frac{1}{2}P+p)$ is the free two-particle propagator. At least in perturbation theory, Eq. (B2) defines a kernel $K(W,p,q)$, including self-mass corrections of the quark propagator, in terms of $G(W,p,q)$. [Equation (B2) is a means to sum up contributions from Feynman diagrams which arise in perturbation theory. It does not imply, of course, that $G(W,p,q)$ has poles corresponding to free quark-antiquark states, as is the case for $G_F(W,p)$. The mass parameters in $G_F(W,p)$ represent effective, constituent quark masses.] The BS equation for the wave function reads

$$\psi(W_n,p)=G_F(W_n,p)\int\frac{d^4q}{(2\pi)^4}\,K(W_n,p,q)\psi(W_n,q)\,. \tag{B3}$$

Equations (B1) and (B2) imply the normalization condition

$$\int\frac{d^4p}{(2\pi)^4}\,\frac{d^4q}{(2\pi)^4}\,\bar{\psi}(W_n,p)\,\frac{\partial}{\partial W_n}\,[G_F^{-1}(W_n,p)(2\pi)^4\delta^4(p-q)-K(W_n,p,q)]\times\psi(W_n,q)=1\,. \tag{B4}$$

In general it will be necessary to employ perturbation theory[59] to calculate $\psi(W_n,p)$. Writing the kernel as

$$K\equiv K_0+\delta K\,, \tag{B5}$$

one obtains

$$\psi(W_n,p)=\psi_0(W_n,p)\left(1+\int\frac{d^4q}{(2\pi)^4}\,\frac{d^4q'}{(2\pi)^4}\,\bar{\psi}_0(W_n,q)\,\frac{\partial}{\partial W_n}\,\delta K(W_n,q,q')\psi_0(W_n,q')\right)+\int\frac{d^4q}{(2\pi)^4}\,\frac{d^4q'}{(2\pi)^4}\,\hat{G}_0(W_n,p,q)\delta K(W_n,q,q')\psi_0(W_n,q')+O(\delta K^2)\,, \tag{B6}$$

where

$$\hat{G}(W,p,q)=G_0(W,p,q)-\frac{\psi_0(W_n,p)\bar{\psi}_0(W_n,q)}{W-W_n-i\epsilon}\,. \tag{B7}$$

ψ_0 and G_0 represent wave function and Green's function corresponding to K_0 [the superscript "0" for the unperturbed energy eigenvalues W_n^0 has been dropped in Eqs. (B6) and (B7)].

The success of the potential model for quarkonia suggests that a natural choice for K_0 is an instantaneous kernel of the general form

$$K_0(W,p,q)=\sum_i\,V^i(W,(\vec{p}-\vec{q})^2,\vec{p}^{\,2},\vec{q}^{\,2})\Gamma_i^{(1)}\Gamma_i^{(2)}, \tag{B8}$$

where $\Gamma_i^{(1)}$ ($\Gamma_i^{(2)}$) are Dirac matrices acting on the particle (antiparticle) spinor indices. The quark propagator reads

$$S(p)=\frac{\Lambda_+(\vec{p})\gamma_0}{p_0-E_p+i\epsilon}+\frac{\Lambda_-(\vec{p})\gamma_0}{p_0+E_p-i\epsilon}\,,$$

where

$$\Lambda_\pm(\vec{p})=\frac{1}{2E_p}\,[E_p\pm H(\vec{p})]\,, \tag{B9}$$

$$E_p=\sqrt{m^2+\vec{p}^{\,2}}\,,\quad H(\vec{p})=\gamma^0(\vec{\gamma}\vec{p}+m)\,.$$

In the nonrelativistic limit one obtains

$$S^{NR}(p)=\frac{(1+\gamma_0)/2}{p_0-m-(\vec{p}^{\,2}/2m)+i\epsilon}-\frac{(1-\gamma_0)/2}{p_0+m+(\vec{p}^{\,2}/2m)-i\epsilon}\,. \tag{B10}$$

Correspondingly, the BS equation for the wave function becomes

$$\psi_0^{\mathrm{NR}}(W_n,p)=\frac{1}{[p_0+W_n-m-(\vec{p}^{\,2}/2m)+i\epsilon][p_0-W_n+m+(\vec{p}^{\,2}/2m)-i\epsilon]}$$
$$\times\int\frac{d^4q}{(2\pi)^4}\sum_i V_{\mathrm{NR}}^i(W,(\vec{p}-\vec{q})^2,\vec{p}^{\,2},\vec{q}^{\,2})\left(\frac{1+\gamma_0}{2}\right)^{(1)}\Gamma_i^{(1)}\psi_0^{\mathrm{NR}}(W_n,q)\Gamma_i^{(2)}\left(\frac{1-\gamma_0}{2}\right)^{(2)} \tag{B11}$$

as in the nonrelativistic limit only the large (small) components of the particle (antiparticle) part of the wave function survive. Equation (B11) implies that the scalar wave function $\phi_n(\vec{p})$, defined by

$$\int\frac{dp_0}{2\pi}\psi_0^{\mathrm{NR}}(W_n,p)\equiv\phi_n(\vec{p})\chi_n\,, \tag{B12}$$

obeys the Schrödinger equation

$$\left(2m+\frac{\vec{p}^{\,2}}{m}-2W_n\right)\phi_n(\vec{p})+\int\frac{d^3p}{(2\pi)^3}V(|\vec{p}-\vec{q}|)\phi_n(\vec{q})=0 \tag{B13}$$

if the nonrelativistic limit of the kernel satisfies the condition

$$\sum_i V_{\mathrm{NR}}^i(W,(\vec{p}-\vec{q})^2,\vec{p}^{\,2},\vec{q}^{\,2})\left(\frac{1+\gamma_0}{2}\Gamma_i\frac{1+\gamma_0}{2}\right)^{(1)}\left(\frac{1-\gamma_0}{2}\Gamma_i\frac{1-\gamma_0}{2}\right)^{(2)}=V(|\vec{p}-\vec{q}|)\left(\frac{1+\gamma_0}{2}\right)^{(1)}\left(\frac{1-\gamma_0}{2}\right)^{(2)} \tag{B14}$$

[Eq. (B14) is obviously fulfilled by the frequently employed linear combination of vector and scalar exchange]. $V(|\vec{p}-\vec{q}|)$ is the phenomenological potential used to calculate the quarkonium spectrum [thus the nonrelativistic limit of the BS kernel K_0 determines the $(Q\bar{Q})$ mass spectrum up to relativistic v^2/c^2 corrections]; for a general combination of singlet and triplet states the spinor part χ in Eq. (B12) is conveniently written as

$$\chi=\frac{1}{\sqrt{2}}\frac{1+\gamma_0}{2}(a\gamma_5+b\not{s})\,,\quad a^2+b^2=1 \tag{B15}$$

where $s^\mu=(0,\vec{s})$ represents the spin polarization in the c.m. system. The BS wave function $\psi_0^{\mathrm{NR}}(W_n,p)$ reads

$$\psi_0^{\mathrm{NR}}(W_n,p)=\frac{2W_n-2m-(\vec{p}^{\,2}/m)}{[p_0+W_n-m-(\vec{p}^{\,2}/2m)+i\epsilon][p_0-W_n+m+(\vec{p}^{\,2}/2m)-i\epsilon]}\,\phi_n(\vec{p})\chi_n\,. \tag{B16}$$

The normalization condition Eq. (B4) corresponds to

$$\int\frac{d^3p}{(2\pi)^3}\phi_n^*(\vec{p})\phi_n(\vec{p})=1\,. \tag{B17}$$

In order to obtain the leptonic width one has to calculate the amplitude

$$\Gamma_{n\mu}=-ie_Q\int\frac{d^4p}{(2\pi)^4}\,\mathrm{tr}[\gamma_\mu\psi(W_n,p)]\,, \tag{B18}$$

which, in powers of δK, is given by [Eqs. (B6) and (B7)]

$$\Gamma_{n\mu}=-ie_Q\int\frac{d^4p}{(2\pi)^4}\,\mathrm{tr}[\gamma_\mu\psi_0(W_n,p)]\left(1+\int\frac{d^4q}{(2\pi)^4}\frac{d^4q'}{(2\pi)^4}\bar{\psi}_0(W_n,q)\frac{\partial}{\partial W_n}\delta K(W_n,q,q')\psi_0(W_n,q')\right)$$
$$-ie_Q\int\frac{d^4p}{(2\pi)^4}\frac{d^4q}{(2\pi)^4}\frac{d^4q'}{(2\pi)^4}\,\mathrm{tr}[\gamma_\mu\hat{G}_0(W_n,p,q)\delta K(W_n,q,q')\psi_0(W_n,q')]+O(\delta K^2)$$
$$\equiv-ie_Q(\Gamma_{n\mu}^{(0)}+\Gamma_{n\mu}^{(1)}+\cdots)\,. \tag{B19}$$

e_Q denotes the electric charge of the quark. In the nonrelativistic limit we immediately obtain $\Gamma_{n\mu}^{(0)}$ (cf. Fig. 16),

$$\Gamma_{n\mu}^{(0)\mathrm{NR}}=\int\frac{d^4p}{(2\pi)^4}\,\mathrm{tr}[\gamma_\mu\psi_0^{\mathrm{NR}}(W_n,p)]$$
$$=\sqrt{2}\,s_\mu\phi_n(0)\,. \tag{B20}$$

The first-order correction in δK is given by

$$\Gamma_{n\mu}^{(1)}=\int\frac{d^4p}{(2\pi)^4}\frac{d^4q}{(2\pi)^4}\frac{d^4q'}{(2\pi)^4}$$
$$\times\,\mathrm{tr}[\gamma_\mu\hat{G}_0(W_n,p,q)\delta K(W_n,q,q')\psi_0(W_n,q')]\,. \tag{B21}$$

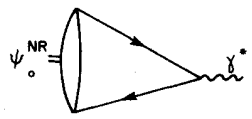

FIG. 16. Lowest-order amplitude for leptonic width [cf. Eq. (B.20)].

Here we have neglected the derivative term in Eq. (B19). To leading order in α_s, to which we will confine ourselves in the following discussion, this term is only a counterterm[60]; beyond the leading order in α_s this contribution is included in the estimate of the uncertainties in Sec. III.

The integrations in Eqs. (B19) and (B21) involve all momentum transfers $(q-q')^2$ which occur in the kernel $\delta K(W_n, q, q')$. For small momentum transfers the wave functions occuring in $\hat{G}_0$ can be treated nonrelativistically. Overlap integrals, such as

$$\int \frac{d^4q}{(2\pi)^4}\,\frac{d^4q'}{(2\pi)^4}\,\bar{\psi}_0(W_n, q)\delta K(W_n, q, q')\psi_0(W_n, q'),$$

vanish in this kinematical regime as, by definition, δK approaches zero in the nonrelativistic limit. Therefore small momentum transfers do not contribute to the integrals in Eqs. (B19) and (B21). For large momentum transfers $\hat{G}_0$ cannot be treated nonrelativistically. But now one can neglect binding corrections and calculate the contribution to the corresponding integrals in perturbation theory. Replacing $\hat{G}_0$ by G_F and using the BS equation for the subtraction term involving K_0, one obtains

$$\Gamma^{(1)}_{n\mu} = \int \frac{d^4p}{(2\pi)^4}\,\frac{d^4q}{(2\pi)^4}\,\mathrm{tr}[\gamma_\mu G_F(W_n, p)K(W_n, p, q)\psi_0(W_n, q)] + \int \frac{d^3p}{(2\pi)^3}\,\frac{d^3q}{(2\pi)^3}\,\frac{1}{2m + (\vec{p}^{\,2}/m) - 2W_n} \times V(|\vec{p}-\vec{q}|)\phi_n(\vec{q})\,\mathrm{tr}[\gamma_\mu \chi_n]. \tag{B22}$$

To leading order in α_s, $K(W_n, p, q)$ and $V(|\vec{p}-\vec{q}|)$ are given by

$$K(W_n, p, q) \sim 4\pi\alpha_s C_2(R)\gamma_\mu^{(1)}\gamma_\nu^{(2)} D^{\mu\nu}(p-q, \lambda^2, \xi), \tag{B23a}$$

$$D_{\mu\nu}(k) = \left(g_{\mu\nu} + \xi\,\frac{k_\mu k_\nu}{k^2 + i\epsilon}\right)\frac{(-i)}{k^2 - \lambda^2 + i\epsilon},$$

$$V(|\vec{p}-\vec{q}|) \sim -\frac{4\pi\alpha_s C_2(R)}{|\vec{p}-\vec{q}|^2 + \lambda^2}. \tag{B23b}$$

Using Eqs. (B23) the nonrelativistic, zero-binding limit of Eq. (B22) reads (cf. Fig. 17)

$$\Gamma^{(1)}_{n\mu} = 4\pi\alpha_s C_2(R)\phi_n(0)\left\{-\int \frac{d^4p}{(2\pi)^4}\,\mathrm{tr}[\gamma_\nu S(-\tfrac{1}{2}P_n + p)\gamma_\mu S(\tfrac{1}{2}P_n + p)\gamma_\lambda \chi_n]D^{\nu\lambda}(p^2, \lambda, \xi) - \int \frac{d^3p}{(2\pi)^3}\,\frac{1}{(\vec{p}^{\,2}/m)(\vec{p}^{\,2} + \lambda^2)}\,\mathrm{tr}[\gamma_\mu \chi_n]\right\}. \tag{B24}$$

The integrals are readily evaluated, yielding

$$\Gamma^{(1)}_{n\mu} = \sqrt{2}\, s_\mu\,\frac{\alpha_s}{2\pi}\,C_2(R)\phi_n(0)\left[\ln\frac{\Lambda}{m} - \frac{7}{4} + 2\pi\,\frac{m}{\lambda} + 2\ln\frac{\lambda}{m} + \xi\left(\ln\frac{\Lambda}{m} - \ln\frac{\lambda}{m}\right) - 2\pi\,\frac{m}{\lambda} - L^{(1)}\right], \tag{B25}$$

where $L^{(1)}$ is the counterterm arising from self-mass insertions on the quark lines and the derivative term in Eq. (B19),

$$L^{(1)} = \ln\frac{\Lambda}{m} + \frac{9}{4} + 2\ln\frac{\lambda}{m} + \xi\left(\ln\frac{\Lambda}{m} - \ln\frac{\lambda}{m}\right). \tag{B26}$$

Equations (B25) and (B26) yield the final result $[C_2(R) = \frac{4}{3}]$

$$\Gamma_{n\mu} = \sqrt{2}\, s_\mu \phi_n(0)\left(1 - \frac{8\alpha_s}{3\pi} + \cdots\right), \tag{B27}$$

implying immediately the familiar correction factor Eq. (3.2) for the leptonic widths, first obtained by Barbieri *et al.*, based on the QED calculation of Karplus and Klein.[29]

Relativistic corrections to Eq. (B27) will have at least three different origins: (1) v^2/c^2 corrections to $\Gamma^{(0)}_{n\mu}$, (2) v^2/c^2 corrections to the perturbative part of $\Gamma^{(1)}_{n\mu}$, and (3) nonperturbative v^2/c^2 contributions due to differences between

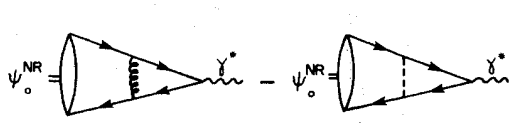

FIG. 17. First-order QCD correction to lowest-order amplitude for leptonic width [cf. Eq. (B.24)]. The wiggly line indicates an exchanged gluon, the dashed line the Coulombic interaction.

K and K_0 for small momentum transfers. Given a particular Lorentz structure of K_0, the corrections of type (1) can be calculated in a straightforward way. However, the task to evaluate the corrections of types (2) and (3) appears to be rather hopeless. In particular, the type (2) corrections are not of relative order $\alpha_s v^2/c^2$, as one might naively expect, but rather proportional to $\alpha_s v/c$,[61] and therefore cannot be neglected compared to the corrections to $\Gamma^{(0)}_{n\mu}$.

In summary, the first-order QCD corrections to the Van Royen–Weisskopf formula appear to be a reliable estimate of radiative corrections. In particular, they are independent of the Lorentz structure of the zeroth-order BS kernel, as they involve only its nonrelativistic limit, i.e., the $(Q\bar{Q})$ potential. On the other hand, a complete treatment of the relativistic corrections appears to be impossible without a much deeper understanding of bound states in QCD.

---

*Operated by Universities Research Association, Inc. under contract with the United States Department of Energy.

[1]J. J. Aubert *et al.*, Phys. Rev. Lett. 33, 1404 (1974); J.-E. Augustin *et al.*, *ibid.* 33, 1406 (1974); G. S. Abrams *et al.*, *ibid.* 33, 1453 (1974).

[2]T. Appelquist and D. H. Politzer, Phys. Rev. Lett. 34, 43 (1975).

[3]E. Eichten, K. Gottfried, T. Kinoshita, J. Kogut, K. D. Lane, and T. M. Yan, Phys. Rev. Lett. 34, 369 (1975).

[4]S. W. Herb *et al.*, Phys. Rev. Lett. 39, 252 (1977); W. R. Innes *et al.*, *ibid.* 39, 1240 (1977); K. Ueno *et al.*, *ibid.* 42, 486 (1979).

[5]C. Berger *et al.*, Phys. Lett. 76B, 243 (1978); C. W. Darden *et al.*, *ibid.* 76B, 246 (1978); 76B, 364 (1978); 80B, 419 (1979); J. Bienlein *et al.*, *ibid.* 78B, 360 (1978); C. Berger *et al.*, Z. Phys. C 1, 343 (1979).

[6]D. Andrews *et al.*, Phys. Rev. Lett. 44, 1108 (1980); T. Bohringer *et al.*, *ibid.* 44, 1111 (1980); D. Andrews *et al.*, *ibid.* 45, 219 (1980); G. Finocchiaro *et al.*, *ibid.* 45, 222 (1980).

[7]CLEO Collaboration, Cornell Report No. CLNS-80/464, 1980 (unpublished); G. Mageras *et al.*, Phys. Rev. Lett. 46, 1115 (1981) (CUSB Collaboration).

[8]For recent reviews, see C. Quigg, in *Proceedings of the 1979 International Symposium on Lepton and Photon Interactions at High Energies, Fermilab,* edited by T. B. W. Kirk and H. D. I. Abarbanel (Fermilab, Batavia, Illinois, 1980); K. Gottfried, in *High Energy e^+e^- Interactions*, proceedings of the International Symposium, Vanderbilt University, Nashville, Tennessee, 1980 edited by R. S. Panvini and C. S. Csoma (AIP, New York, 1980); K. Berkelman, in *High Energy Physics—1980,* proceedings of the XXth International Conference, Madison, Wisconsin, edited by L. Durand and L. G. Pondrom (AIP, New York, 1981).

[9]General reviews of the theory are given in T. Appelquist, R. M. Barnett, and K. D. Lane, Annu. Rev. Nucl. Sci. 28, 387 (1978); M. Krammer and H. Krasemann, in *New Phenomena in Lepton-Hadron Physics,* edited by D. Fries and J. Wess (Plenum, New York and London, 1979); J. D. Bjorken, in *Quantum Chromodynamics,* proceedings of the Summer Institute on Particle Physics, SLAC, 1979, edited by Anne Mosher (SLAC, Stanford, 1980); J. L. Rosner, lectures at Advanced Studies Institute on Techniques and Concepts of High Energy Physics, St. Crox, Virgin Islands, 1980 (unpublished).

[10]C. Quigg and J. L. Rosner, Phys. Rep. 56, 167 (1979).

[11]H. Grosse and A. Martin, Phys. Rep. 60, 341 (1980); R. A. Bertlmann and A. Martin, Nucl. Phys. B168, 111 (1980).

[12]A. Martin, Phys. Lett. 93B, 338 (1980); Report No. TH.2980-CERN, 1980 (unpublished). For earlier work on power potentials, see M. Machacek and Y. Tomozawa, Ann. Phys. (N.Y.) 110, 407 (1978); C. Quigg and J. L. Rosner, Comments Nucl. Part. Phys. 8, 11 (1978).

[13]W. Buchmüller, G. Grunberg, and S.-H. H. Tye, Phys. Rev. Lett. 45, 103 (1980); 45, 587(E) (1980).

[14]G. Bhanot and S. Rudaz, Phys. Lett. 78B, 119 (1978).

[15]E. Eichten, K. Gottfried, T. Kinoshita, K. D. Lane, and T. M. Yan, Phys. Rev. D 17, 3090 (1978); 21, 203 (1980).

[16]The flavor independence of the static potential has been demonstrated in a model-independent way by use of the inverse-scattering method. For a recent review and references, see C. Quigg and J. L. Rosner, in *High Energy Physics—1980* (Ref. 8).

[17]A representative list includes W. Celmaster, H. Georgi, and M. Machacek, Phys. Rev. D 17, 879 (1978); W. Celmaster and F. S. Henyey, *ibid.* 18, 1688 (1978); A. Billoire and A. Morel, Nucl. Phys. B135, 131 (1978); B. Margolis, R. Roskies, and N. De Takacsy, paper submitted to the IV European Antiproton Conference, Barr, France, 1978 (unpublished); J. L. Richardson, Phys. Lett. 82B, 272 (1979); R. D. Carlitz, D. B. Creamer, and R. Roskies (unpublished); R. D. Carlitz and D. B. Creamer, Ann. Phy. (N.Y.) 118, 429 (1979); R. Levine and Y. Tomozawa, Phys. Rev. D 19, 1572 (1979); 21, 840 (1980); J. Rafelski and R. D. Viollier, Report No. TH.2673-CERN, 1979 (unpublished); MIT Reports Nos. CTP 791 and 819, 1979 (unpublished); G. Fogleman, D. B. Lichtenberg, and J. G. Wills, Lett. Nuovo Cimento 26, 369 (1979); B. R. Zhou, Univ. of Hofei report (unpublished).

[18]The $\overline{\text{MS}}$ scheme was introduced in W. A. Bardeen, A. Buras, D. W. Duke and T. Muta, Phys. Rev. D 18, 3998 (1978). For a review, see A. Buras, Rev. Mod. Phys. 52, 199 (1980). The relations between Λ_{MS}, (minimal subtraction), $\Lambda_{\overline{\text{MS}}}$ (modified minimal subtraction), and Λ_{mom} (momentum space) read $\Lambda_{\text{MS}} = 0.377\Lambda_{\overline{\text{MS}}}$, $\Lambda_{\text{mom}} = 2.16\Lambda_{\overline{\text{MS}}}$. See W. Celmaster and R. J. Gonsalves, Phys. Rev. Lett. 42, 1435 (1979); Phys. Rev. D 20, 1420 (1979).

[19]C. Quigg and J. L. Rosner, Phys. Lett. 71B, 153 (1977); M. Machacek and Y. Tomozawa, Prog. Theor. Phys. 58, 1890 (1977); Ann. Phys. (N.Y.) 110, 407

(1978).
[20]The importance of the leptonic widths as a means to distinguish the different types of potentials has also been emphasized on the basis of the inverse-scattering formalism. See Quigg and Rosner, Ref. 16.
[21]W. A. Bardeen and A. Buras, private communication.
[22]We follow the notation of Gross and Wilczek, Phys. Rev. Lett. 30, 1343 (1973). For SU(3) one has $C_2(G) = 3$; N_f is the number of flavors.
[23]W. E. Caswell, Phys. Rev. Lett. 33, 244 (1974); D. R. T. Jones, Nucl. Phys. B75, 531 (1974).
[24]W. Fischler, Nucl. Phys. B129, 157 (1977).
[25]A. Billoire, Phys. Lett. 92B, 343 (1980).
[26]We acknowledge clarifying discussions with W. A. Bardeen concerning the importance of classical field configurations.
[27]C. G. Callan, R. F. Dashen, and D. J. Gross, Phys. Rev. D 17, 2717 (1978); Phys. Rev. Lett. 44, 435 (1980).
[28]V. A. Mateev, B. V. Struminskii, and A. N. Tavkhelidze, DUBNA Report No. P-2524, 1965 (unpublished); H. Pietschmann and W. Thirring, Phys. Lett. 21, 713 (1966); R. van Royen and V. F. Weisskopf, Nuovo Cimento 50, 617 (1967).
[29]R. Karplus and A. Klein, Phys. Rev. 87, 848 (1952); R. Barbieri, R. Gatto, R. Kögerler, and Z. Kunzst, Phys. Lett. 57B, 455 (1975).
[30]J. D. Jackson, in *Weak Interactions at High Energy and the Production of New Particles*, proceedings of the Summer Institute on Particle Physics, SLAC, 1976, edited by M. C. Zipf (SLAC, Stanford, 1977). Recent contributions include H. J. Schnitzer, Phys. Rev. D 19, 1566 (1979); M. Dine, Phys. Lett. 81B, 339 (1979); E. Eichten and F. L. Feinberg, Phys. Rev. Lett. 43, 1205 (1979); Harvard report, 1980 (unpublished).
[31]K. Königsmann, Crystal Ball Collaboration, SLAC Report No. SLAC-PUB-2594, 1980 (unpublished).
[32]W. Buchmüller, Y. J. Ng, and S.-H. H. Tye, Fermilab Report Pub 81/46, 1981 (unpublished).
[33]E. Eichten and K. Gottfried, Phys. Lett. 66B, 286 (1977).
[34]T. Sterling, Nucl. Phys. B141, 272 (1978).
[35]Particle Data Group, Rev. Mod. Phys. 52, S24 (1980).
[36]For recent work, see G. Karl, S. Meshkov, and J. L. Rosner, Phys. Rev. Lett. 45, 215 (1980); R. McClary and N. Byers, UCLA Report No. UCLA/80/TEP/20, 1980 (unpublished); a novel approach based on QCD sum has recently been suggested by A. Yu. Khodjamirian, Phys. Lett. 90B, 460 (1980); Yerevan Physics Institute report, 1980 (unpublished).
[37]See, for instance, S. Nussinov, Z. Phys. C 3, 165 (1979); A. Martin, in *High Energy Physics—1980* (Ref. 8); R. A. Bertlmann and S. Ono, University of Vienna Report No. UWThPh-80-33, 1980 (unpublished).
[38]For a detailed discussion, see Ref. 25.
[39]W. A. Bardeen and A. Buras, private communication.
[40]R. Barbieri, G. Curci, E. d'Emilio, and E. Remiddi, Nucl. Phys, B154, 535 (1979).
[41]R. Barbieri, M. Caffo, R. Gatto, and E. Remiddi, Phys. Lett. 95B, 93 (1980).
[42]C. Quigg and J. L. Rosner, Phys. Lett. 72B, 462 (1978).
[43]H. Krasemann and S. Ono, Nucl. Phys. B154, 283 (1979).
[44]M. Krammer, H. Krasemann, and S. Ono, DESY Report No. 80/25, 1980 (unpublished).
[45]See, for instance, S. Pakvasa, M. Dechantsreiter, F. Halzen, and D. M. Scott, Phys. Rev. D 2, 2862 (1979); J. Ellis, CERN Reports Nos. 79-01, 615, and 662, 1979 (unpublished); G. Goggi and G. Penso, Nucl. Phys. B165, 429 (1980); I. I. Y. Bigi and H. Krasemann, Z. Phys. C 7, 127 (1981); L. M. Sehgal and P. M. Zerwas, Aachen Report No. PITHA 80-11, 1980 (unpublished); J. H. Kühn, Max-Planck-Institut, Munich Report No. MPI-PAE/PTh 37/80, 1980 (unpublished).
[46]The contribution to the total width from the exchange of a W boson is expected to be negligible. See, for instance, L. Sehgal and P. Zerwas, Ref. 45.
[47]Particle Data Group, Rev. Mod. Phys. 52, S41 (1980).
[48]The calculation of the radiative corrections to the three-gluon quarkonium decay is in progress (P. Mackenzie and G. P. Lepage, private communication).
[49]For a discussion of the scheme dependence of radiative corrections to quarkonium decays, see G. Grunberg, Phys. Lett. 95B, 70 (1980); A. Buras, Report No. Fermilab-Pub-80/43/THY, 1980 (unpublished); P. M. Stevenson, Madison Reports Nos. DOE-ER/0881-153, 1980 and DOE-ER/0881-155, 1980 (unpublished); W. Celmaster and D. Sivers, Report No. ANL-HEP-PR-80-29, 1980 (unpublished).
[50]Hadronic transitions may probe the large- and intermediate-distance regions, Y. P. Kuang and T. M. Yan (unpublished). See also K. Gottfried, Phys. Rev. Lett. 40, 598 (1978); G. Bhanot, W. Fischler, and S. Rudaz, Nucl. Phys. B155, 208 (1979); M. E. Peskin, *ibid.* B156, 365 (1979); T. M. Yan, Phys. Rev. D 22, 1652 (1980); K. Shizuya, University of California Report No. LBL-10714, 1979 (unpublished).
[51]M. A. Shifman, A. I. Vainshtein, and V. I. Zakharov, Nucl. Phys. B147, 385 (1979); B147, 448 (1979). With respect to the size of ϕ, see, however, W. Wetzel, Heidelberg Report No. HD-THEP-79-15, 1980 (unpublished).
[52]H. B. Nielsen and P. Olesen, Nucl. Phys. B160, 380 (1979).
[53]R. Fukuda, Phys. Rev. D 21, 485 (1980); R. Fukuda and Y. Kazama, Phys. Rev. Lett. 45, 1142 (1980).
[54]R. C. Giles and S.-H. H. Tye, Phys. Rev. Lett. 37, 1175 (1976), Phys. Rev. D 16, 1079 (1977); W. Buchmüller and S.-H. H. Tye, Phys. Rev. Lett. 44, 850 (1980). Additional states occur also in the MIT bag model; however, the first few additional states in the MIT bag model have either the wrong quantum numbers or zero wave function at the origin, to be observed in the e^+e^- channel. Hence they cannot be detected in the measurement of R in e^+e^- annihilation, in contrast to "vibrational states." For recent work on additional states in the bag model, see P. Hasenfratz, R. R. Horgan, J. Kuti, and J. M. Richard, Phys. Lett. 95B, 299 (1980).
[55]M. Creutz, Phys. Rev. D 21, 2308 (1980); K. G. Wilson, Cornell Report No. CLNS 80/442, 1980 (unpublished); J. B. Kogut, R. B. Pearson, and J. Shigemitsu, Phys. Rev. Lett. 43, 484 (1979); G. Mack, DESY Report No. 80/03, 1980 (unpublished).
[56]See, for instance M. Abramowitz and I. A. Stegun, *Handbook of Mathematical Functions* (Dover, New York, 1968).
[57]For a similar expression, see Richardson (Ref. 17).
[58]W. Celmaster, Phys. Rev. D 19, 1517 (1979); L. Berg-

ström, H. Snellman, and G. Tengstrand, Phys. Lett. 80B, 242 (1979); 82B, 419 (1979); Z. Phys. C 4, 215 (1980); E. C. Poggio and H. J. Schnitzer, Phys. Rev. D 20, 1175 (1979); 21, 2034 (1980); C. Michael and F. P. Payne, Phys. Lett. 91B, 441 (1980).

[59]For a recent treatment of perturbation theory in the BS formalism, see G. P. Lepage, Phys. Rev. A 16, 863 (1977); SLAC Report No. 212, 1978 (unpublished); G. T. Bodwin and D. R. Yennie, Phys. Rep. 43, 267 (1978); G. Feldman, T. Fulton, and D. L. Heckathorn, Nucl. Phys. B167, 364 (1980).

[60]The importance of derivative terms in the renormalization of BS amplitudes has been discussed in W. Buchmüller and E. Remiddi, Nucl. Phys. B162, 250 (1980).

[61]For positronium, the corresponding corrections have recently been evaluated: W. E. Caswell and G. P. Lepage, Phys. Rev. A 18, 810 (1979); W. Buchmüller and E. Remiddi, Nuovo Cimento 60A, 109 (1980).